Integrative biology defines novel biomarkers of resistance to strongylid infection in horses

Guillaume Sallé[1,*], Cécile Canlet[2], Jacques Cortet[1], Christine Koch[1], Joshua Malsa[1], Fabrice Reigner[3], Mickaël Riou[4], Noémie Perrot[4], Alexandra Blanchard[5], Nuria Mach[6]

[1], INRAE, Université de Tours, UMR 1282 Infectiologie et Santé Publique, F-37380 Nouzilly, France

[2], INRAE, Université de Toulouse, ENVT, INP-Purpan, UPS, UMR 1331 Toxalim, F-31027 Toulouse, France

[3], INRAE, UE 1297 Physiologie Animale de l'Orfrasière, F-37380 Nouzilly, France

[4], INRAE, UE 1277 Plateforme d'infectiologie expérimentale, F-37380 Nouzilly, France

[5], Pancosma, Rolle, Switzerland

[6], Université Paris-Saclay, INRAE, AgroParisTech, Génétique Animale et Biologie Intégrative, 78350 Jouy-en-Josas, France

*, Corresponding author

Email: Guillaume.Salle@inrae.fr

Abstract

The widespread failure of anthelmintic drugs against nematodes of veterinary interest requires novel control strategies. Selective treatment of the most susceptible individuals could reduce drug selection pressure but requires appropriate biomarkers of the intrinsic susceptibility potential. To date, this has been missing in livestock species. Here, we selected Welsh ponies with divergent intrinsic susceptibility to cyathostomin infection and found that their potential was sustained across a 10-year time window. Using this unique set of individuals, we monitored variations in their blood cell populations, plasma metabolites and faecal microbiota over a grazing season to isolate core differences between their respective responses under worm-free or natural infection conditions. Our analyses identified the concomitant rise in plasmatic phenylalanine level and faecal *Prevotella* abundance and the reduction in circulating monocyte counts as biomarkers of the need for drug treatment. This biological signal was replicated in other independent populations. We also unravelled an immunometabolic network encompassing plasmatic beta-hydroxybutyrate level, short-chain fatty acid producing bacteria and circulating neutrophils that forms the discriminant baseline between susceptible and resistant individuals. Altogether our observations open new perspectives on the susceptibility of equids to cyathostomin infection and leave scope for both new biomarkers of infection and nutritional intervention.

Keywords

horse; nematode; cyathostomin; gut microbiota; metabolomic; ^{1}H-NMR; blood; neutrophil; 16S

Introduction

Infection by gastro-intestinal nematodes is a major burden for human development worldwide as they both affect human health[1] and impede on livestock production[2]. Worldwide reports of anthelmintic drug failures against nematodes of veterinary importance have accumulated[3], threatening the sustainability of livestock farming in some areas. The same pattern applies in horses whereby widespread benzimidazole failure and intermediate pyrantel efficacy against cyathostomin populations have been reported[4–6]. These small strongyles locate in their host hindgut and are responsible for growth retardation in young animals[7,8]. The massive emergence of developing larval stages from the caeco-colic mucosa can cause a larval cyathostominosis syndrome[9] that remains a leading cause of parasite-mediated death[10].

Factors contributing most to the selection of drug-resistant cyathostomin populations in equids remain uncertain[4,5]. However, significant and heritable inter-individual variation in resistance to strongylid infection has been reported in both domestic[11,12] and wild horse populations[13]. This variation leaves scope for restricting drug application to the most susceptible horses, thereby alleviating the selection pressure on parasite populations. To date, the genetic architecture of this trait has not been defined in equids, although indications from ruminant species would be in favour of a polygenic architecture[14–16] defining a stronger type 2 cytokinic polarization in resistant individuals[17,18].

Identifying biomarkers of this intrinsic resistance potential would both contribute to understanding the host-parasite relationship and to defining relevant biomarkers for use in the field. Current targeted-selective treatment schemes are based on faecal egg count (FEC) that has suboptimal sensitivity and remains time-consuming despite recent advances that should ease egg detection[19]. As a result, its uptake in the field varies widely across countries and remains limited[5,20] despite being cost-effective[21,22]. To date, limited alternative biomarkers have been identified. Alteration in serum albumin level and decrease in circulating fructosamine were the main features found in cyathostomin infected ponies[23]. Independent

observations concluded that mixed strongyle infection was associated with mild inflammatory perturbations[24]. We previously highlighted that susceptible ponies had lower monocyte but higher lymphocyte counts than resistant individuals upon natural strongylid infection[25]. More susceptible individuals also exhibited differential modulation of their faecal microbiota, including enrichment for the *Ruminococcus* genera[25], corroborating independent observations of alterations in the gut microbiota composition of infected horses[25–28].

In horses as in other host-parasite systems, limited efforts have been made to isolate compositional shifts in plasma metabolites following parasite nematode infection. Beyond murine models of helminth infection[29,30], implementation of this technology could define a urinary biomarker of infection by *Onchocerca volvulus* in humans[31]. This was however not reproduced in other cohorts of patients[32]. In livestock species, a single study has applied metabolomic profiling on horse faecal matter to identify biomarkers of infection by parasitic nematodes but found little differences between horses with contrasted levels of strongylid infection[26].

In any case, these observations remain limited to individual host compartments and do not provide an integrated perspective of the physiological underpinnings associated with susceptibility to infection. Because we are aiming to distinguish between individuals before the onset of degraded clinical signs, the biological signals may be subtle. To this respect, integration of systems biology data - that consider multiple high-dimensional measures from various host compartments - is expected to better identify the multiple features defining a given physiological state[33].

Under this assumption, we combined and analysed metabolomic, metagenomic and clinical data collected on a selected set of intrinsically resistant and susceptible ponies to identify the physiological components underpinning their resistance potential. Our data defined a strongylid infection signature built around lower circulating monocytes, enriched plasmatic phenylalanine concentration and higher *Prevotella* load in faecal microbiota that we could replicate in independent populations. We also identified an immunometabolic signature

96 centered on neutrophils that best discriminated between resistant and susceptible individuals
97 across strongyle-free or natural infection conditions. These results begin to define the
98 physiological bases supporting the intrinsic resistance potential to strongylid infection in
99 equids.
100

Results

This experiment was based on a set of individual Welsh ponies with divergent resistance potential to strongylid infection. During the experiment (2015), we produced metabolomic data that we present herein and integrated this plasma-related dataset with previously described faecal bacteria profiles and clinical parameters[25]. We analysed the data produced for each group under worm-free conditions (day 0) or following natural infection (day 132) to i) identify biomarkers of infection, ii) establish a holistic view of the physiological underpinnings of the resistance potential to strongyle infection in horses.

1. Pony divergence toward strongyle infection is significant and sustained

We selected 20 female Welsh ponies with divergent susceptibility to strongylid infection. Their susceptibility potential was predicted from their past FEC history (at least three FEC records over two years between 2010 and 2015). During the experiment (2015) and following natural infection (day 132), 17 ponies displayed FEC values in good agreement with their predicted potential. In that case, 8 of the susceptible ponies (**TS**) had FEC above the considered 200 eggs/g cut-off for treatment (average FEC = 419 ± 149 eggs/g) at day 132, and 9 resistant ponies (**TR**) were below this threshold (average FEC = 56 ± 77 eggs/g). Our prediction hence achieved an accuracy of 85%. Other ponies that did not match expectations had either higher susceptibility (850 eggs/g for the predicted resistant individual) or too low FEC (0 and 50 eggs/g for the two susceptible individuals).

In agreement with this observation, FEC measured in the TS and TR ponies during the five years preceding the experiment departed significantly from the herd mean (0.6 standard deviations ; $P = 0.01$ and $P = 0.02$ for TS and TR groups respectively; Fig 1). To ensure that their intrinsic potential was true, we compared their FEC records collected after the experiment took place (between 2015 and 2020) to that of their herd (1,436 individual records). We confirmed that their divergence was sustained (-0.76 and +0.63 standard deviation from mean in TS and TR ponies respectively; $P = 0.02$ in both cases) throughout the following years

(Fig 1), hence validating their intrinsic potential. This corresponded to an average FEC of 43 eggs/g (min = 0; max = 2,200 eggs/g) and 756 eggs/g (min = 0; max = 2,800 eggs/g) in TR and TS ponies respectively, while the average herd FEC was 320 eggs/g (min = 0; max = 5,400 eggs/g).

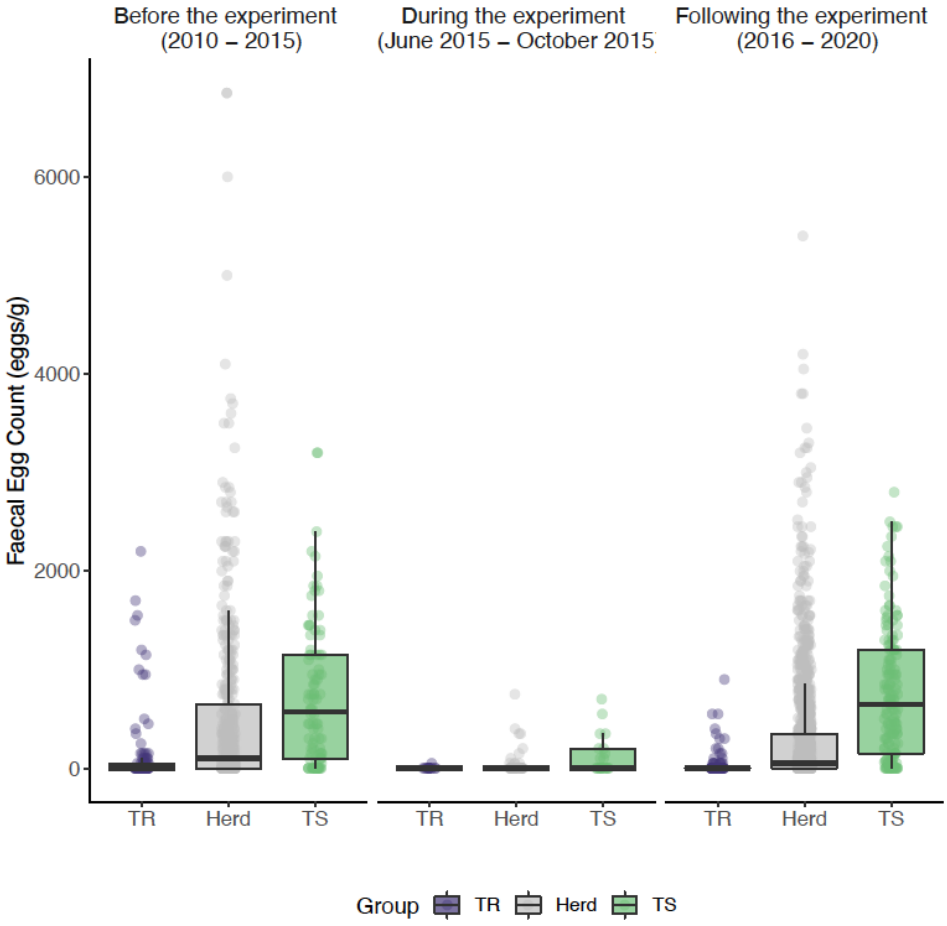

Figure 1. FEC-informed pony potential prediction is robust through time

The distribution of observed Faecal Egg Counts before the experiment (2010-2015), during the experiment (2015) and after the experiment (2015-2020) in the predicted susceptible (8 individuals, 271 records; green) and resistant (9 individuals, 223 records; purple) ponies and their herd unselected counterparts (127 individuals, 1,436 measures; grey) is represented. Dots stand for individual measures and boxplots represent the data distribution (mean materialized by a vertical bar within the box that stands for the 25% to 75% interquartile range).

2. Metabolomic profiling highlights the association between plasmatic phenylalanine level and FEC

To identify markers of pony intrinsic resistance potential, we measured variation in their plasma metabolites using ^{1}H-NMR between worm-free conditions (day 0) and after natural infection (day 132). This metabolomic profiling of TR and TS ponies throughout the grazing seasons found a total of 791 metabolic buckets, corresponding to 119 unique metabolite signals (Fig 2, supplementary Table 1). These included several amino acids, energy metabolism-related metabolites, saccharides, unknown lipids, and organic osmolytes in the plasma. Among these signals, we observed 29 unassigned bins in three main windows ranging between 1.115 and 1.435 ppm, 3.385 and 4.305 ppm or 6.805 and 7.895 ppm (supplementary Table 1).

The ANOVA – simultaneous component analysis (ASCA) applied to metabolomic time series data identified significant temporal variation ($P < 0.001$) but no differential rewiring occurred between TR and TS pony metabolomes ($P = 0.54$). The temporal variation was structured around five signals (supplementary Fig 1) associated with alkalene moieties from lipids (^{1}H-NMR signal at 5.265–5.355 ppm), sugar moieties of α- and β-glucose (3.455–3.555 ppm) in overlap with proline (3.395–3.445 ppm) and branched-chain amino-acids (BCAAs) such as valine (1.045–1.055 ppm) and leucine (0.965-0.975 ppm). These signals showed mean leverage of 3.4% (ranging between 1.5% and 7.8%) and squared prediction error below 2.2 x 10^{-5}. Among these, the high-intensity signals ascribable to glucose decreased between the strongyle-free (day 0) and strongyle-infected (day 132) conditions (supplementary Fig 1).

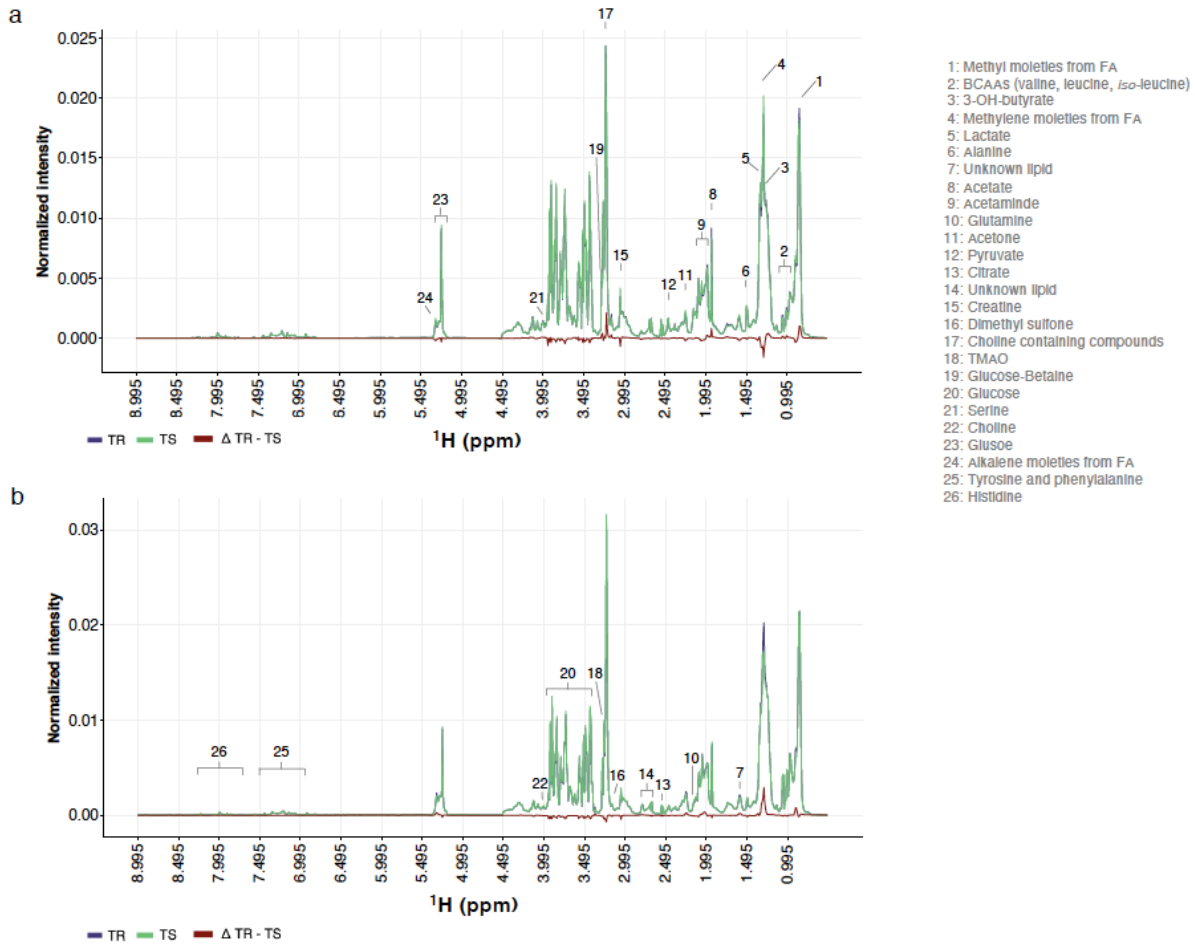

Figure 2. Representative ^{1}H-NMR spectra measured in resistant and susceptible ponies

Group average ^{1}H-NMR signal intensities are plotted against the considered chemical shifts ranging from 0.995 to 8.995 ppm and overlaid for resistant (TR; purple) and susceptible (TS; green) pony groups at day 0 (strongyle-free; panel a) or day 132 (strongyle infected; panel b). Differential intensity between groups is drawn in red. Associated metabolites are annotated by numbers.

Despite the lack of systematic modifications of metabolomes between TR and TS ponies, we sought to identify individual metabolites that would reflect the intrinsic susceptibility status of ponies before any infection took place (day 0) or metabolites that would differentiate individuals in need of treatment at the end of the grazing season (day 132). Considering the nominal *P*-values of 5%, we identified differences in dimethyl-sulfone and lysine associated signals that were all decreased in the TS pony group (supplementary Fig 2a). None of these

174 signals were however significantly correlated with final FEC measured at day 132 (Spearman's
175 ρ ranging between -0.08 and 0.34, supplementary Fig 2b).

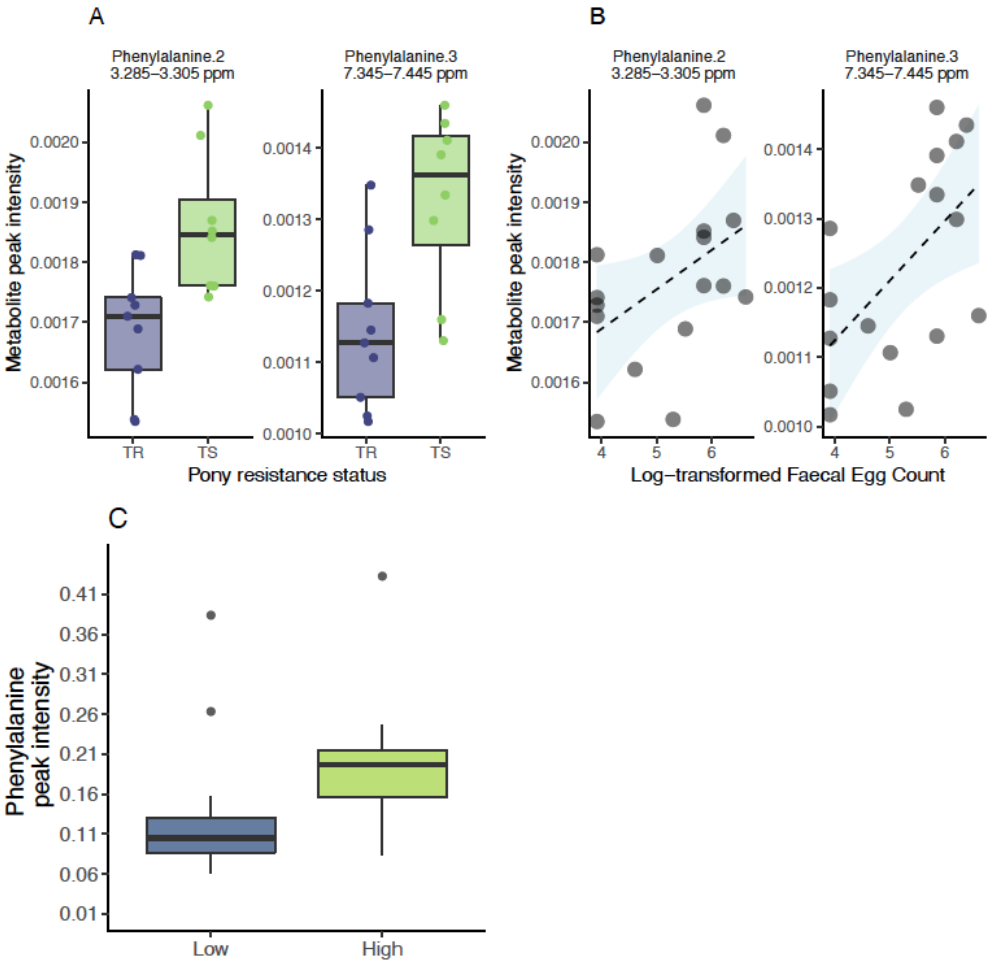

176

177 **Figure 3. Differential metabolites between infected resistant and susceptible ponies (day 132)**
178 Panel A shows metabolite signal intensity distribution in each pony susceptibility group (purple:
179 resistant, TR; green: susceptible, TS) at day 132. Panel B shows the relationship between these
180 metabolite signal intensities (X-axis) at day 0, and matching log-transformed Faecal Egg Count (Y-axis)
181 at day 132. Panel C describes observed phenylalanine levels in the faecal matter of an independent
182 cohort of British horses with low or high FEC [26].

183

184 The same approach applied to TR and TS ponies after natural infection at day 132 found
185 lower levels of phenylalanine (^{1}H-NMR signals at 3.285-3.305 ppm and 7.345-7.445 ppm) in
186 TR compared to TS ponies (nominal P-value = 6 x 10^{-3}). In addition, an unidentified metabolite
187 between 6.815-6.815 ppm (U13) was significantly lower in TR (P = 0.04). Phenylalanine signal

188 intensities increased with FEC (Spearman's ρ ranging between 0.55 and 0.60, $P< 0.05$, n =
189 17). Using the faecal metabolomic data from another independent set of British horses [26], we
190 could validate this signal. In that study and in line with our results, faecal phenylalanine level
191 was significantly increased in horses with higher FEC (*Wilcoxon's test = 27*, *P-value* = 0.02,
192 Fig 3C).
193 Altogether these results indicate that strongylid infection experienced by TR and TS ponies
194 did not induce metabolome-wide modifications. However, phenylalanine was the most
195 discriminant between TR and TS ponies under infection and stands as a biomarker of the
196 need for treatment.
197

198 ## 3. Multi-compartment data integration identifies circulating monocytes,
199 ## phenylalanine and faecal *Prevotella* levels as discriminant features under
200 ## infection

201 To mine the physiological differences between infected TR and TS ponies deeper, we applied
202 a data integration framework (sGCC-DA) bringing together clinical, metabolomic and
203 previously analyzed faecal microbiota data from these individuals [25]. The first component of
204 the sGCC-DA better discriminated between TR and TS ponies and retained nine clinical
205 parameters, 15 bacterial genera and ten plasma metabolite signals (Fig 3, supplementary Figs
206 3 and 4).
207 The network of correlations between these features was structured around two major clusters
208 (Fig 4, supplementary Figs 3 and 4). A first core of features built around average daily gain
209 (ADG) and four commensal gut bacterial genera (*Anaerovibrio, Fibrobacter, Prevotella,* and
210 *Treponema*) displayed higher levels in TR ponies under infection (Fig 4, supplementary Figs 3
211 and 4). These features were negatively correlated to a strongylid susceptibility-associated
212 cluster that encompassed neutrophil counts (2.8 ± 0.51 and 3.05 ± 0.8 million cells/mm^3 in
213 TR and TS ponies), the haematocrit (average of 38.74% ± 1.7 vs. 41.45% ± 4.1 in TR and TS

ponies) and the plasmatic levels of serine and essential amino acids such as phenylalanine, lysine and tryptophan (Fig 4, supplementary Figs 3 and 4). This underscores the association between phenylalanine and FEC (Fig 3b, c).

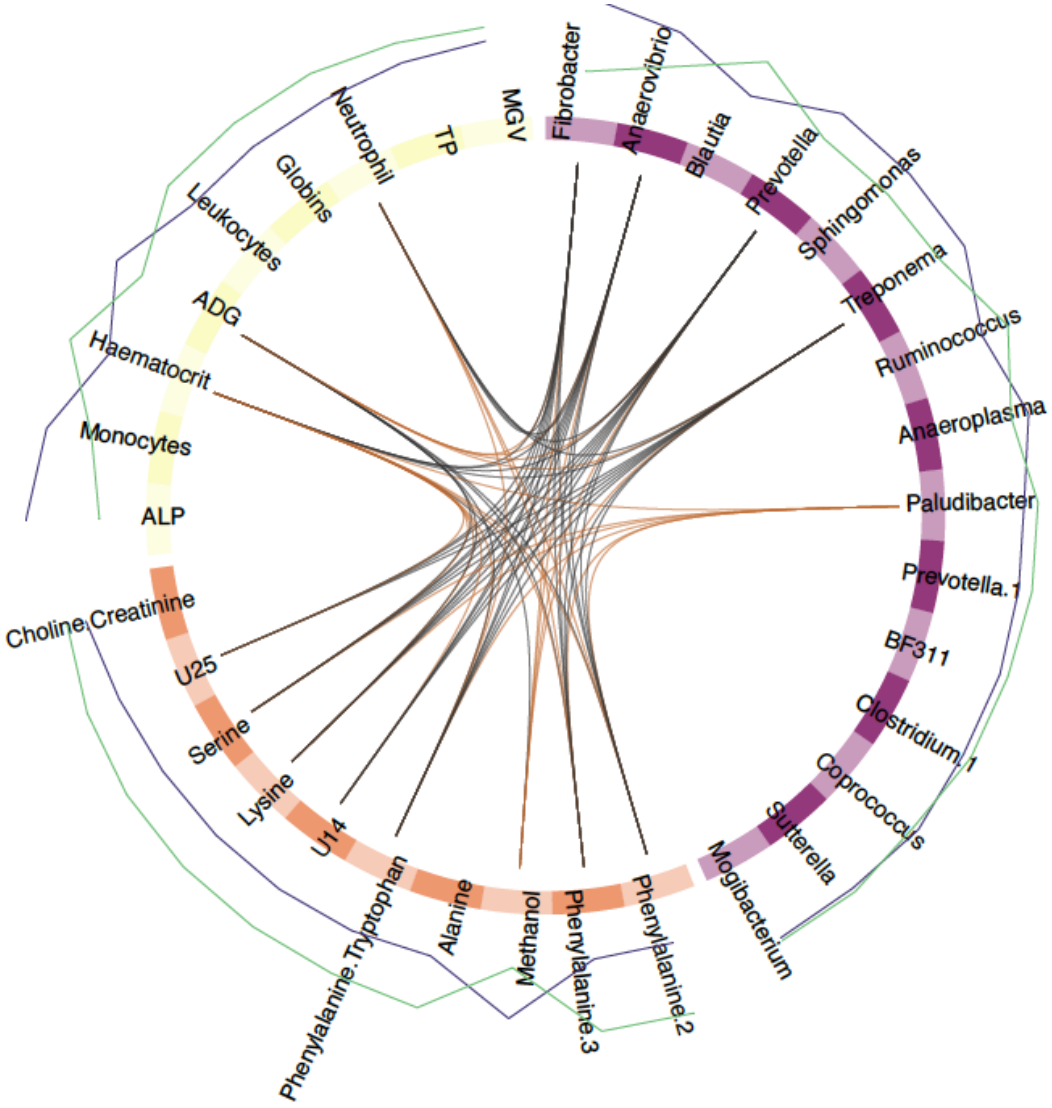

Figure 4. Circos plot showing features best discriminating between infected resistant and susceptible ponies (day 132)

For each of the three input data types (clinical data in yellow, bacterial genera in purple and metabolite signals in orange), the features best discriminating between resistant and susceptible ponies are listed. A link is materialized between two features if their shared correlation is above 0.45 (chocolate if positive, grey otherwise). External green and purple lines represent the relative feature level in each pony susceptibility group (resistant, TR: purple; susceptible, TS: green). MGV: Mean Globular Volume; TP: Total Protein; ALP: Alkaline Phosphatase; U14, U25: Unknown metabolites 14 and 25.

Additional features included higher monocyte counts (1.178 ± 0.23 and 1.038 ± 0.24 million cells/mm^3 in TR and TS ponies on average) and higher levels of plasmatic alkaline phosphatase (ALP; 5.39 ± 0.15 and 5.25 ± 0.12 Units/L) in TR ponies (Fig 4). But these parameters displayed least covariation with other parameters (Fig 4).

Analysis for KEGG pathway enrichment of metabolite signals found significant over-representation of Aminoacyl-tRNA biosynthesis (FDR = 1.1 x 10^{-4}) underpinned by the presence of alanine, lysine, phenylalanine, serine, and tryptophan (supplementary Table 2). Of note, alanine and phenylalanine plasmatic levels defined significant enrichment for the dengue fever (supplementary Table 2). The most significant enrichment was defined by the *Blautia*, *Coprococcus* and *Ruminococcus* association found in forms of pediatric Crohn's disease (FDR = 2.5 x 10^{-3}). Two other significant enrichments included infection-mediated perturbations associated with the HIV-1 virus in humans (underpinned by *Anaerovibrio* and *Clostridium* genera, FDR = 1.12 x 10^{-4}) or with murine model of *Plasmodium* infection (underpinned by *Anaeroplasma* and *Clostridium*, FDR = 0.05).

To validate the association of the most discriminant blood and bacterial features with FEC, we used either a previously published horse data set [26] for bacterial count, or additional blood samples taken from 25 strongylid infected ponies in 2020 (Fig 5). Out of the five most discriminating bacterial genera identified by our sGCC-DA approach under infection at day 132, *Prevotella* (FDR = 0.19; nominal *P-value* = 0.04) also showed significant differences in their mean abundances between Peachey et al.'s horses with low or higher FEC (Fig 5). Monocyte counts were also negatively correlated with FEC levels in the independent set of ponies (Spearman's ρ = -0.31, *P-value* = 0.14; Fig 5).

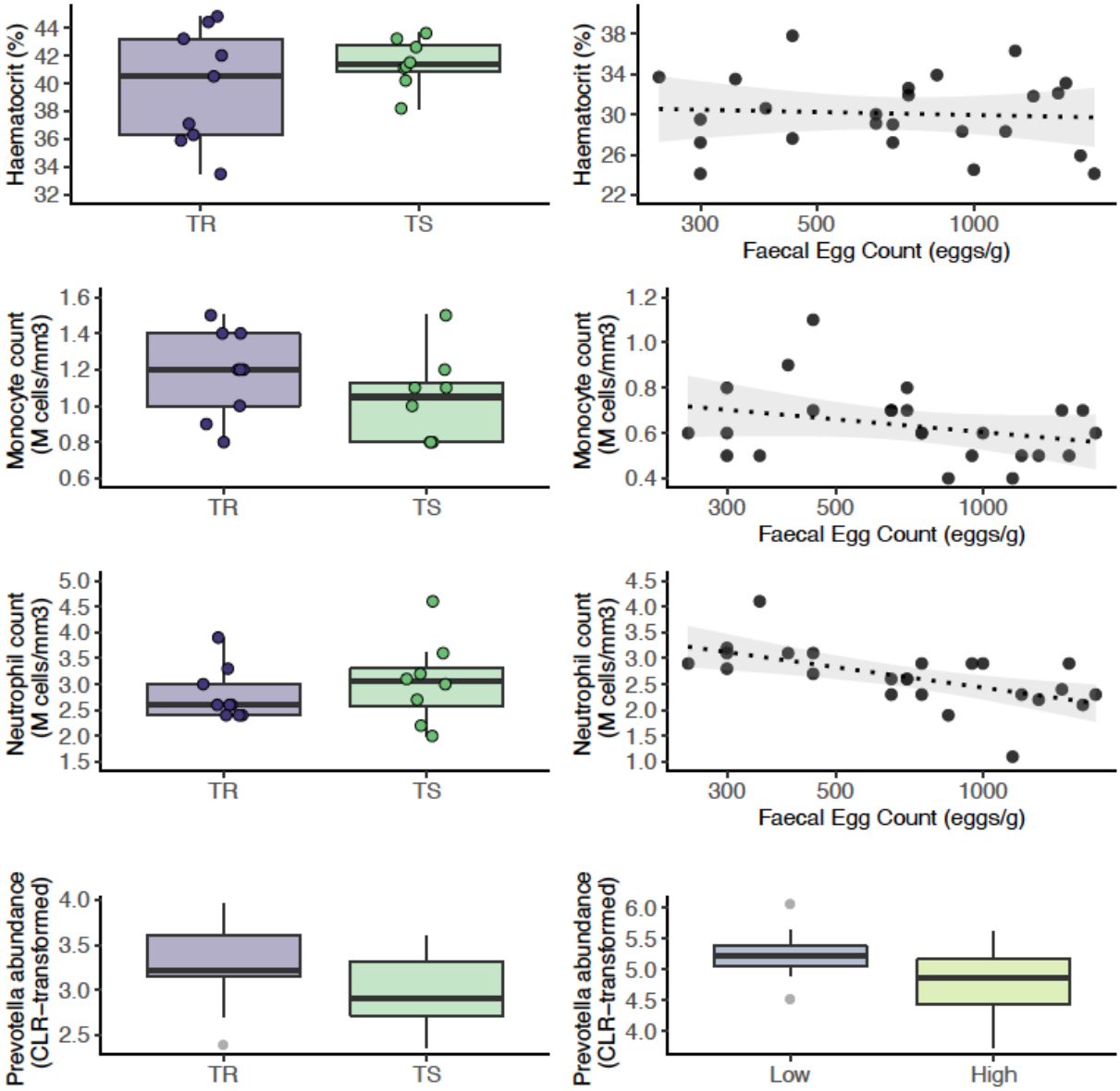

Figure 5. Validation of the most discriminant features between resistant and susceptible ponies under strongylid infection

Each row presents the feature level in resistant and susceptible ponies (left panels) and the association with Faecal Egg Count recorded in an independent set of ponies or horses (for the *Prevotella* genus). CLR: Centered Log-Transformed. The figure highlights the significant positive relationship between circulating monocyte count and faecal abundance of the *Prevotella* genus in independent individuals.

The trend was however opposite for the neutrophil population (Spearman's ρ = -0.63, *P-value* = 9 x 10^{-4}; Fig 5) and no relationship between FEC and haematocrit was found in this independ set of individuals (Spearman's ρ = -0.07, *P-value* = 0.7; Fig 5).

These findings hence retain increased *Prevotella* abundance in faecal material as a conserved signal in equids with reduced FEC, and monocyte counts appears to be a good predictor of FEC level.

4. Short-chain fatty acid producing bacteria, plasmatic lysine and circulating neutrophils recapitulate pony intrinsic potential across conditions

Using the same analytical framework, we aimed to identify features that would best define the intrinsic pony resistance potential across worm-free or natural infection conditions.

The sGCC-DA applied on records measured under worm-free conditions (day 0) identified reduced circulating neutrophil and leukocyte counts in the TR ponies as the most discriminant clinical parameters (supplementary Figs 5, 6, and 7). Cell counts of these two populations were tightly linked with plasmatic levels of 1-methylhistidine (7.785 ppm; reduced in TR ponies), lysine (1.445-1.465 and 1.845-1.915 ppm; increased in TR ponies) and β-hydroxybutyrate (4.125-4.135 ppm; increased in TR ponies). In addition to these parameters, maximal covariance was obtained for a few genera from the Actinomycetia class (order Corynebacteriales), namely *Dietzia*, *Gordonia*, *Mycobacterium* and *Sacharopolyspora* (order Pseudonocardiales), that all showed higher relative abundances in resistant ponies, as well as the candidate genera BF311 within Bacteroidetes (e.g., *BF311*; supplementary Figs 5). On the opposite, higher relative abundance of butyrate-producing Clostridia, specifically *Anaerofustis, Coprococcus* and *Ruminococcus* were found in TS ponies (supplementary Figs 5). These genera showed positive correlations with circulating lymphocytes and neutrophil counts (ranging between 0.51 and 0.68 for lymphocyte counts and between 0.38 and 0.51 for neutrophil counts respectively; supplementary Figs 5 and 7). Of note, the presence of

283 *Prevotella* and *Desulfovibrio* among the set of covarying features defined significant
284 enrichments compatible with *Plasmodium* infection in mice or *Schistosoma haematobium*
285 infection in humans (FDR = 0.04 in both cases; supplementary Table 2).
286 Combining these differential features between pony groups under worm-free conditions with
287 that found after strongylid infection retained a core set of seven markers consistently
288 discriminating TR and TS ponies across infection conditions (supplementary Fig 8). For these
289 markers, we aimed to identify differential trends between both groups across infection
290 conditions.
291 First, circulating neutrophil and leukocyte counts showed significant increase following
292 infection (P = 0.02 and 4 x 10^{-4} respectively), but this increase was not different between TR
293 and TS ponies (P = 0.5 in both cases; supplementary Fig 8 and supplementary Table 3). This
294 trend was also not corroborated in another independent set of individuals (Fig 5).
295 Second, plasmatic lysine level was significantly different between infected TR and TS ponies
296 (P = 0.002) and matched independent observations made in faecal samples from another
297 cohort of British horses (Fig 6). Our temporal records also supported a differential decrease
298 of plasmatic lysine levels between TR and TS ponies from worm-free to natural infection
299 conditions (P = 0.02).

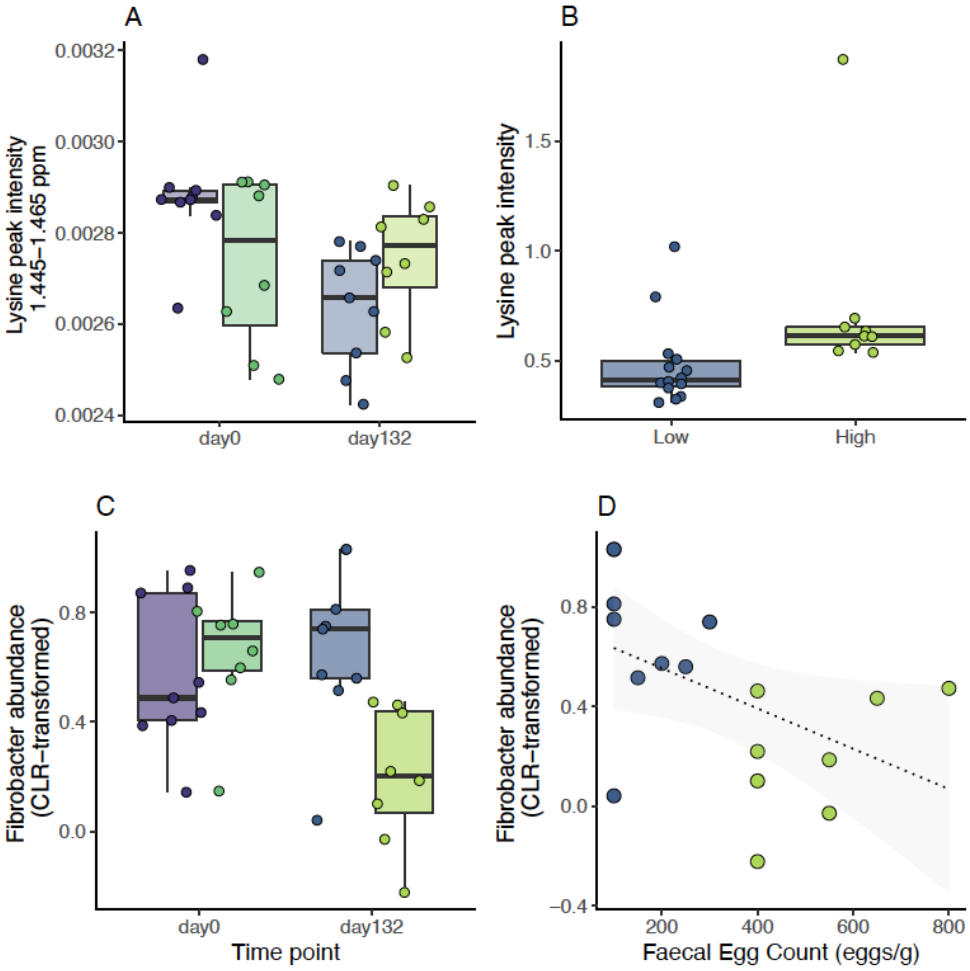

Figure 6. Discriminant features between resistant and susceptible ponies across infection conditions

Measured values of lysine signal intensity (A) and Fibrobacter abundance (C) are plotted across susceptibility groups (TR: resistant, in blue; TS: susceptible, in green) and time points (day0: before infection; day132: under strongylid infection, 132 days after the onset of grazing season). Lysine intensity measured on faecal material in an independent cohort of British horses with low or high Faecal Egg Count is represented in panel B. Panel D shows the relationship between Fibrobacter count in TR and TS ponies at day 132 and measured FEC.

Third, sGCC-DA recognized three dominant gut bacteria, namely *Fibrobacter, Ruminococcus,* and *Treponema*, and one rare microbial taxa (*Coprococcus*) as keystone species whose covariation formed a distinct signature between the two pony groups (Fig 6, supplementary Fig 8). Using linear regression modeling, we found a significant decrease in faecal abundance of *Treponema* (P = 1.7 x 10^{-2}) upon infection that was shared across pony groups (supplementary Fig 8). On the contrary, the observed rise in *Fibrobacter* abundance at day

132 was slightly milder in the TS ponies (-0.73 ± 0.26, FDR = 4.4 x 10^{-2}; Fig 4, supplementary Table 3).

Lysine and *Fibrobacter* would hence mark the intrinsically higher sensitivity of TS ponies.

Discussion

Inter-individual variation in susceptibility to strongylid infection offers the opportunity to reduce drug selection pressure by selectively treating the most susceptible individuals. To date, the physiological markers associated with this resistance potential are to be defined. Here, we selected resistant and susceptible ponies and confirmed that their potential was sustained over a 10-year time window. Using this unique set of individuals, we performed the first detailed investigations of the variations occurring in three different compartments (blood, plasma and faeces) to identify the underpinnings of their differential resistance to strongylid. Our findings are two-fold. First, we found support for defining phenylalanine, circulating monocytes and faecal abundance of *Prevotella* as biomarkers of strongylid infection in equids. Second, we identified an immunometabolic network encompassing beta-hydroxybutyrate level, short-chain fatty acid producing bacteria and circulating neutrophils that recapitulates the intrinsic resistance potential of ponies under both worm-free and natural infection conditions.

Elevation of plasmatic phenylalanine concentration has long been recognized as a metabolic consequence of bacterial and viral infections[34]. Similar observation has also been made in the faecal matter of infected horses[26] and we could replicate it from plasmatic samples. Of note, our data highlighted the covariation of this essential amino acid with average daily gain and the concomitant increase in plasmatic alkaline phosphatase concentration. This is compatible with strongyle infection reducing muscle protein synthesis (in line with observed reduced average daily gain), thereby increasing the extracellular release of phenylalanine and its subsequent uptake by the liver (whose activity was tracked by the increased alkaline phosphatase level). This model would match the theoretical framework derived from other infectious processes[34]. Altogether, plasmatic phenylalanine represents another diagnostic option for strongylid infection. The sensitivity and specificity of this marker remains to be

347 determined in a larger cohort for field use in association with monocyte count and faecal
348 *Prevotella* abundance.
349 The concomitant increase in the plasmatic level of this aromatic amino acid with the monocyte
350 count decrease upon infection in susceptible individuals also opens new perspectives on the
351 pathophysiology associated with strongylid infection in equids. Indeed, observations in
352 humans demonstrated that D-phenyllactic acid - an antibacterial compound derived from
353 phenylalanine and produced by the gut microflora - can activate the hominid-specific
354 Hydroxy-Carboxylic Acid (HCA) 3 G-protein coupled receptor expressed by monocytes,
355 thereby favoring their recruitment[35]. While the only lactate-associated HCA1 receptor exists
356 in equids, the possibility remains that phenylalanine derivatives could recruit immune cells[36].
357 Under this speculative model, serum phenylalanine (increased in infected individuals), would
358 enter the gut lumen before subsequent transformation into phenyllactic acid by gut bacteria.
359 Bacteria-derived phenyllactic would then be absorbed into the portal vein and serve as a
360 recruitment signal for circulating monocytes. Further studies on this receptor would confirm
361 its role in any differential immunometabolic regulations between the resistant and susceptible
362 pony groups.
363 Under infection, susceptible individuals exhibited decreased abundance of faecal *Prevotella*.
364 Effects of the *Prevotella* genus are still debated[37]. Experimental colonization of germ-free mice
365 by *Prevotella* promoted the decrease of IL-18 interleukin expression, neutrophil recruitment
366 at the site of infection and gut inflammation[37]. *Prevotella* was also associated with
367 susceptibility to *Plasmodium* infection in mice[38], increased in patients infected by the human
368 trematode *S. haematobium*[39] and in the colon of pigs infected by *Trichuris suis*[40]. A *Prevotella*-
369 led inflammatory state would hence define the reduced strongyle infection observed in
370 resistant ponies. This would contradict past findings in mice showing the detrimental
371 association between IL-18 and *Trichuris muris* infection[41]. Because this cytokine seems to be
372 sensitive to its environment, there is scope for microbiota-based regulations[42] that would
373 differ between resistant and susceptible individuals.

In our attempt to discriminate between resistant and susceptible ponies, we identified a feature network with contrasted proinflammatory abilities. First, resistant ponies exhibited higher plasmatic lysine levels across conditions. Lysine is an essential amino acid for metabolism and immune response. Although the role of its derivative on the immune system is yet to be clarified[43], it is a natural ligand of the GPRC6 receptor[44] that can modulate Th-2 response and antibody production by B cells[45]. Second, butyrate-producing bacteria and other bacteria able to metabolize β-hydroxybutyrate into butyrate (e.g. *Coprococcus*) defined differential baselines between pony susceptibility groups under worm-free conditions. The former is known to favour an anti-inflammatory state by inhibiting the neutrophil inflammasome and the release of pro-inflammatory cytokines like IL-1β and IL-18[46,47]. Butyrate binds free fatty acid receptors, like FFAR2 that is enriched on neutrophil cell surface[36], thereby promoting their intestinal recruitment[48]. Third, faecal *Fibrobacter* was a core discriminating feature of the intrinsic resistance potential. The drastic reduction of faecal *Fibrobacter* abundance in susceptible ponies upon strongylid infection mirrored past observations made in pigs infected with *T. suis,* for which the reduction occurred irrespective of the worm load[49]. In goats, abundance of this genus was negatively correlated with the pro-inflammatory cytokines TNFα that is produced by monocytes[50]. *Fibrobacter* bacteria are key cellulose degraders that produce succinate subsequently converted into propionate, another short-chain fatty acid able to modulate the recruitment of monocytes and neutrophils[36]. The reduction of this bacterial genera could hence result in a pro-inflammatory state favourable to the development of strongyle infection in susceptible ponies.

This immuno-metabolic network tying the host metabolites with its gut microbiota also points towards a key role of neutrophils in the definition of strongylid susceptibility. In line with this strand of evidence, we found a consistent covariation between circulating neutrophils and intrinsic susceptibility to strongylid infection. This relationship was however not validated in another independent population with higher excretion levels than that found during our 2015 experiment. The role played by neutrophils hence remains to be fully characterized as for

401 other host-helminth models[51,52]. Transient neutrophilia (in the range of 9 x 10^9 cells per L) was
402 previously described as the only haematological variation in ponies subjected to experimental
403 infection by cyathostomins[23]. But neutrophils are not typically associated with type 2 immunity
404 - that is effective against helminths[53] - and they do not play a role against the infection by
405 *Trichinella spiralis*, a clade I nematode[54]. However, neutrophils can cooperate with
406 macrophages to bring nematode infection under control as found for *Litomosoides*
407 *sigmodontis*[55], *Strongyloides stercoralis*[56] and *Heligmosomoides polygyrus*[57]. They also
408 appear to be regulated by the type-2 cytokinic environment to prevent damages to the host[51].
409 In horses, neutrophils respond to IL-4 stimulation - a type 2 cytokine - by an increase in the
410 pro-inflammatory cytokines TNF-α and IL-8 but a decrease in IL1-β[58] that could be detrimental
411 to the anti-helminth response. The covariation between neutrophil counts and the enhanced
412 susceptibility in horses may thus result from qualitative differences. Application of single-cell
413 RNAseq on neutrophil populations from the two pony backgrounds could provide significant
414 advances in the understanding of their respective properties. Neutrophils were however not
415 part of the recently released equine mononuclear cells atlas[59]. Quantification of cytokines and
416 reactive oxidative species production after *in vitro* exposure to infective strongylid larvae
417 could also unravel distinct properties and putative bias toward a more effective response in
418 resistant individuals.
419 Overall, this work suggests that FEC records from at least two years are sufficient to define
420 the resistance potential of an equid to strongyle infection. It also proposes phenylalanine,
421 monocyte counts and faecal *Prevotella* abundance as biomarkers of infection. Last, we
422 identify a neutrophil-centered network tying together gut microbiota members and a few
423 metabolites as the discriminant baseline between susceptible and resistant individuals. These
424 results open novel perspectives for the understanding of strongylid susceptibility in equids
425 and for nutritional modulation of these infections.
426

Materials and methods

This study relied on measurements previously gathered during the one described previously[25]. Measured features are summarized herein and additional ^{1}H-NMR and FEC parameters collected during this experiment are described. Data were analysed with R version 4.0.2 unless stated otherwise.

Selection and monitoring of 20 ponies with divergent susceptibility profile to strongyle infection.

Ponies were selected from the experimental herd according to their FEC history recorded since 2010. Briefly, individual pony random effect was estimated from individual records after correction for environmental fixed effects including year, season, age at sampling, time since last treatment and last anthelmintic drug received. This was implemented for the only ponies recorded thrice a year, over at least 2 years. Using these estimates, the ten most susceptible and ten most resistant ponies were retained for this study. Median FEC over the past 5 years were 800 and 0 eggs/g for S and R ponies respectively[25]. These two groups of ponies were monitored throughout a grazing season during summer 2015.

To remove any intercurrent nematode infection, ponies were administered moxidectin and praziquantel (Equest Pramox®, Zoetis, Paris, France, 400 µg/kg of body weight of moxidectin and 2,5 mg/kg of praziquantel) three months before the start of the experiment and kept in-door. They were subsequently placed on a 7.44 ha pasture from mid-June to the end of October 2015. To eliminate residual egg excretion observed in some ponies, they were treated with pyrantel (Strongid® paste, Zoetis, Paris, France; single oral dose of 1.36 mg pyrantel base per kg of body weight) 30 days after the onset of pasture season.

To identify blood biomarkers of infection, plasma samples were taken at 0, 24 and 132 days after the start of the trial to compare metabolomes of parasite-free horses (maintained in-door or grazing) with that of infected grazing individuals. These were matched with FEC, average

daily weight gain (ADG), haematological and blood biochemistry parameters and faecal microbiota as previously outlined[25]. Nutritional information has been outlined previously[25].

All experiments were conducted in accordance with EU guidelines and French regulations (Directive 2010/63/EU, 2010; Rural Code, 2018; Decree No. 2013-118, 2013). All experimental procedures were evaluated and approved by the Ministry of Higher Education and Research (APAFIS# 2015021210238289_v4, Notification-1). Procedures involving horses were evaluated by the ethics committee of the Val de Loire (CEEA VdL, committee number 19) and took place at the INRAE, Experimental unit of Animal Physiology of the Orfrasière (UE-1297 PAO, INRAE, Centre de Recherche Val de Loire, Nouzilly, France)

Clinical parameters measurement and modelling

FEC were performed on 5 g of fresh faecal material after intra-rectal sampling and diluted in 70 mL of NaCl solution (d = 1.2) following a modified McMaster technique with a sensitivity of 50 eggs/g[60].

Haematological and serum biochemical parameters were recorded at PFIE (UE-1277 PFIE, INRAE, https://doi.org/10.15454/1.5535888072272498e12). Haematological parameters were determined after 15-min stirring at room temperature with a MS9-5 Haematology Counter® (digital automatic haematology analyzer, Melet Schloesing Laboratories, France). Recorded parameters encompassed erythrocyte, micro- and macro-erythrocyte counts, associated mean corpuscular volume, haematocrit, and mean corpuscular haemoglobin concentration. In addition, circulating thrombocytes were counted as well as leukocytes including lymphocytes, monocytes, neutrophils, basophils and eosinophils. For further analysis, an albumin to globulin ratio (AGR) was also considered.

In addition, serum biochemical parameters were quantified using Select-6V rings with the M-Scan II Biochemical analyser (Melet Schloesing Laboratories, France). These parameters

included albumin, cholesterol, globulin, glucose, alkaline phosphatase (ALP), total proteins (TP) and urea concentrations.

Normality of haematological and biochemistry parameters was tested with the Shapiro-Wilk's test (*shapiro.test()* function in R) and variables showing test value below 0.90, *i.e.* FEC, glucose, ALP and AGR concentrations, and eosinophil count were log-transformed (supplementary Table 4). Validation of monocyte and neutrophil counts were obtained from a group of 25 ponies in October 2020 using the same setting.

Proton Nuclear Magnetic Resonance (^{1}H NMR) data acquisition and processing

Samples were collected in heparin coated tubes. Whole blood drawn for plasma generation was refrigerated immediately at 4°C to minimize the metabolic activity of cells and enzymes and kept the metabolite pattern almost stable. After clotting at 4°C, the plasma was separated from the blood cells and subsequently cryopreserved at -80°C and shipped as a single batch for ^{1}H-NMR profiling. Plasma samples were thawed on ice, 200 µl were mixed with 500 µl of deuterium oxide (D_2O) containing sodium trimethylsilylpropionate (TSP, 1 mM). Samples were vortexed, centrifuged (5,500 g; 10 min; 4°C) and 600 µL of supernatant were transferred into 5 mm NMR tubes.

The ^{1}H-NMR analysis was performed on a Bruker Avance III HD spectrometer (Bruker, Karlsruhe, Germany) operating at 600.13 MHz, and equipped with a 5 mm reversed ^{1}H-^{13}C-^{15}N-^{31}P cryoprobe connected to a cryoplatform. ^{1}H NMR spectra were acquired using a Carr-Purcell-Meiboom-Gill (CPMG) spin echo pulse sequence with a 2-second relaxation delay. The spectral width was set to 20 ppm and 128 scans were collected with 32k points. Free induction decays were multiplied by an exponential window function (LB=0.3 Hz) before Fourier Transform.

Spectra were manually phase and baseline corrected using Topspin 3.2 software (Bruker, Karlsruhe, Germany). All spectra were referenced to TSP (d 0 ppm). The spectral data were

imported in the Amix software (version 3.9, Bruker, Rheinstetten, Germany) to perform data reduction in the region between 9.0 and 0.5 ppm with a bucket width of 0.01 ppm. The region between 5.1 and 4.5 ppm corresponding to water signal was excluded and data were normalized to the total intensity of the spectra.

^{1}H-NMR data were filtered from noise-related signals and finally consisted in 791 buckets ranging from 8.585 to 0.505 ppm (Supplementary Table 1). Buckets were annotated based on similarity of chemical shifts and coupling constants between plasma samples and reference compounds. The comparison was performed between one dimensional analytical data and reference compounds acquired under the same analytical conditions in our internal database, as well as from public databases like the Human Metabolome Database (HMDB, http://hmdb.ca/) and the Biological Magnetic Resonance Data Bank (http://www.bmrb.wisc.edu/). Manually curation was performed to isolate buckets corresponding to the same metabolite. Intensities of these metabolite-specific buckets were summed together to define metabolite-associated signals (hereafter referred to as "signals"), yielding 119 signals for further analysis.

To prevent spurious signals linked to age differences between individuals, metabolite levels at D0 were regressed upon pony age. None of the 119 metabolite signal intensities showed variation associated with pony ages at the considered cut-off (FDR < 5%).

16S faecal microbiota data for data integration

Total microorganism's DNA was extracted from aliquots of frozen fecal samples (200 mg), using E.Z.N.A.® Stool DNA Kit (Omega Bio-Tek, Norcross, Georgia, USA). The V3-V4 16S rRNA gene amplification and sequencing have been described elsewhere[25].

For data integration purpose (described in next paragraph), 16S rRNA gene sequencing data generated from these ponies were re-analysed using qiime2 v.2020.2[61]. Adapter and primers were removed from sequencing data using cutadapt v2.1[62]. Trimmed data was subsequently

imported into qiime2, and denoised using the Divisive Amplicon Denoising Algorithm from dada2[63]. In this workflow, Operational Taxonomic Units (OTU, sequence cluster defined by their dissimilarity level) are replaced by so-called amplicon sequence variant (ASV) that matches observed genetic variation in bacterial 16S rRNA gene amplicons instead of relying on a clustering operation[64]. Reads were quality filtered (maximal expected error of 1 for both reads), chimera trimmed (following the default "consensus" option) and the reads trimmed (6 and 20 bp for forward and reverse reads respectively) to yield 3,054,206 reads. ASVs were subsequently filtered to retain that found in at least two individuals and supported by five reads, before alignment and phylogeny building with mafft and fasttree respectively. ASVs were subsequently assigned taxonomy using a naive Bayes classifier trained on the green genes reference database (gg_13_8) clustered at 99% similarity. This workflow left 6,208 ASVs that were aggregated to 91 genera with phyloseq (v.1.32) for subsequent analysis. Total sum scaling normalization was applied to each taxa abundances for subsequent data integration analysis.

The raw sequences of the gut metagenome 16S rRNA targeted locus are available in NCBI under the Sequence Read Archive (SRA), with the BioProject number PRJNA413884 and SRA accession numbers from SAMN07773451 to SAMN07773550.

Statistical analysis and data integration

Our experiment focused on R and S ponies monitored during a pasture season. Using this experimental design, we interrogated their respective metabolomes 1) to characterize metabolite trajectories throughout a pasture season, 2) to identify biomarkers that would predict the pony intrinsic resistance potential, 3) to identify biomarkers that could be used to differentiate between ponies reaching FEC cut-off for anthelmintic treatment at the end of pasture season. We restricted this analysis to ponies whose predicted resistance status matched the observed FEC value at the end of pasture season, leaving nine true R (**TR**) and

555 eight true S (**TS**) ponies respectively. Statistical analyses applied for each of these three
556 objectives are presented below.

557 ***Multivariate analysis of longitudinal metabolomic data in TR and TS ponies***

558 First, we aimed to characterize metabolomic modifications occurring in TR and TS ponies
559 throughout a grazing season. To analyse our longitudinal data, we implemented an ANOVA-
560 Simultaneous Component Analysis (ASCA)[65,66] with the MetaboAnalyst R package v.3.0.3[67].
561 This analysis first partitions the variance contained in the metabolite data across the factors
562 of interest (susceptibility group and time point including 0, 24 or 132 days after onset of the
563 pasture season) and their interactions, thereby correcting the data for these effects.
564 Simultaneously, a PCA is applied to each partition for dimensionality reduction ultimately
565 isolating the metabolites contributing most to each effect. Significance of each effect was
566 tested by 1,000 permutations. Following ASCA, 37 outlier metabolite signals were identified
567 and subsequently removed from further data integration analysis leaving 319 signals for
568 subsequent analysis.

569 ***Differential analysis of signal metabolite intensities between TR and TS ponies and***
570 ***between ponies in need of treatment***

571 Second, we aimed to identify biomarkers that would either be predictive of the intrinsic
572 resistance potential of an individual (TR vs. TS comparison at day 0) or would distinguish
573 between individuals in need of treatment (TR vs. TS comparison at day 132). To fulfill these
574 two aims, we respectively performed Student's *t* tests on the 319 retained metabolite signals
575 between TR and TS pony baselines or between individuals showing FEC below or above 200
576 eggs/g at day 132. To account for multiple testing, nominal *P*-values were adjusted using the
577 Benjamini-Hochberg correction (FDR) as implemented in the *p.adjust* function (stats package
578 v.4.0.2). Spearman's correlations were estimated using the *rcorr* function from the Hmisc
579 package v.4.4-1[68].

580 ***Data integration to identify biomarkers predictive of parasite resistance or need of***
581 ***treatment***

As a complementary approach for biomarker identification, clinical (including blood cell population profile, blood biochemistry and average daily weight gain), metabolomic (319 signals) and faecal microbiota data were integrated to identify correlated signals associated with intrinsic resistance potential or need of treatment. This approach also has the potential to uncover biological signals that would be missed when considering each dataset independently[33]. We ran two analyses to extract the features from each dataset with best discriminant ability between TR and TS ponies either before the pasture season on one hand, or between TR and TS ponies in need of treatment at day 132 on the other hand.

In this analysis, ASV counts estimated from faecal microbiota data were aggregated at the genus level within each time point of interest (day 0 or day 132) using the *tax_glom* function of the phyloseq package v.1.32.0. They were then filtered to retain those reaching 5% prevalence (n = 45 and 41 at day 0 and day 132 respectively), and normalized with the centered log-ratio transformation of the mixOmics package[69]. ^{1}H NMR data consisted in the 319 metabolite signal intensities retained following filtering and outlier identification with ASCA. Clinical data consisted of 18 parameters. At day 0, ADG was not considered as no variation occurred leaving 17 parameters. FEC was not considered as it was used to define the groups to be compared.

Data integration was performed following the DIABLO (data integration analysis for biomarker discovery using latent variable approaches for Omics studies) framework[70] as implemented in the mixOmics package v.6.12.2. This algorithm implements a sparse generalized canonical correlation discriminant analysis (sGCC-DA)[33,70]. Briefly, DIABLO performs feature selection, thereby retaining the only bacterial genera, metabolite signal or clinical parameters with best discriminative ability between groups. Using this sparse dataset, DIABLO then seeks for latent components (linear combinations of features from each dataset, i.e. ^{1}H-NMR, faecal microbiota, and clinical parameters) that simultaneously explains as much as possible of the covariance between input datasets and the status of interest, *i.e.* pony resistance potential before or under infection[33,70]. We applied this analysis to discriminate between TR and TS

ponies either before the onset of pasture season (day 0) or at pasture turnout (day 132). In each case, the number of features to be retained was determined by cross-validation analysis (10 x 5-fold) with the *tune.block.splsda()* function exploring grids of 10 to 20 genera with increments of 5, 10 to 80 metabolite signals with increments of 10 and 5 to 10 clinical parameters with increment of 1. The correlation matrix between each input datasets was determined after running a partial least square analysis using the *pls()* function[69].

Following data integration, we applied linear regression models to quantify group and time variation in the levels of seven features that distinguished between TR and TS ponies both at day 0 and day 132. These most discriminant features had either an absolute contribution of 0.25 on the first sGCC-DA axis. For metabolite signal intensities, no metabolite matched this condition and all features contributing to the 1st axis at day 0 and 132 were retained.

Enrichment analysis

To isolate biological pathways associated with discriminant ^{1}H NMR signals and bacterial taxa, enrichment analyses were run using the MetaboAnalyst v5.0[67] and MicrobiomeAnalyst[67] web interfaces respectively. Significant metabolite signals were tested for enrichment against KEGG annotated metabolites and disease related blood biomarkers, while enrichment analysis on discriminant bacterial genera were run using taxa collections associated with aging or disease. Any enrichment with a False Discovery Rate (FDR) below 5% was deemed significant.

Validation in an independent set of data

We validated our biological signal on microbial and metabolomic data using the data from Peachey et al.[26] as an independent data set because they combined both 16S rRNA gene amplicon sequencing with metabolomic analyses. While they performed ^{1}H-NMR on faecal

material, we wanted to evaluate how our results obtained from blood ^{1}H-NMR could match theirs. Raw data were retrieved and processed as ours, but following Peachey et al.' read truncation parameters[26]. This process left 3,305,166 sequences assigned to 5,233 ASVs. ASV counts per sample and ASV taxonomic assignments from Clark et al. 2018 and Peachey et al. 2019 are available under the github repository.

Blood parameters of interest were validated in an independent set of 24 ponies with high FEC (821 eggs/g on average, ranging between 250 and 1700 eggs/g). Increased alkaline phosphatase had already been described in infected horses and was not considered for validation.

Data availability statement

R script is available under the https://github.com/guiSalle/STROMAEQ repository and associated data matrices will be made available upon manuscript acceptance. ^{1}H-NMR Data will be deposited on Metabolomicsworkbench.org upon manuscript acceptance. The raw sequences of the gut metagenome 16S rRNA targeted locus are available in NCBI under the Sequence Read Archive (SRA), with the BioProject number PRJNA413884 and SRA accession numbers from SAMN07773451 to SAMN07773550.

References

1. G. B. D. DALYs & Hale Collaborators. Global, regional, and national disability-adjusted life-years (DALYs) for 333 diseases and injuries and healthy life expectancy (HALE) for 195 countries and territories, 1990-2016: a systematic analysis for the Global Burden of Disease Study 2016. *Lancet* **390**, 1260–1344 (2017).
2. Nieuwhof, G. J. & Bishop, S. C. Costs of the major endemic diseases of sheep in Great Britain and the potential benefits of reduction in disease impact. *Anim. Sci.* **81**, 23–29 (2005).
3. Kaplan, R. M. & Vidyashankar, A. N. An inconvenient truth: Global worming and anthelmintic resistance. *Vet Parasitol* **186**, 70–78 (2012).
4. Nielsen, M. K. *et al.* Anthelmintic efficacy against equine strongyles in the United States. *Vet Parasitol* **259**, 53–60 (2018).
5. Sallé, G. *et al.* Risk factor analysis of equine strongyle resistance to anthelmintics. *Int J Parasitol Drugs Drug Resist* **7**, 407–415 (2017).
6. Tzelos, T. *et al.* Strongyle egg reappearance period after moxidectin treatment and its relationship with management factors in UK equine populations. *Vet Parasitol* **237**, 70–76 (2017).
7. Debeffe, L. *et al.* Negative covariance between parasite load and body condition in a

668 population of feral horses. *Parasitology* **143**, 983–97 (2016).
669 8. Rubenstein, D. I. & Hohmann, M. E. Parasites and Social Behavior of Island Feral
670 Horses. *Oikos* **55**, 312 (1989).
671 9. Giles, C. J., Urquhart, K. A. & Longstaffe, J. A. Larval cyathostomiasis (immature
672 trichonema-induced enteropathy): a report of 15 clinical cases. *Equine Vet J* **17**, 196–
673 201 (1985).
674 10. Sallé, G. *et al.* Compilation of 29 years of postmortem examinations identifies major
675 shifts in equine parasite prevalence from 2000 onwards. *Int. J. Parasitol.* (2020)
676 doi:10.1016/j.ijpara.2019.11.004.
677 11. Kornaś, S. *et al.* Estimation of genetic parameters for resistance to gastro-intestinal
678 nematodes in pure blood Arabian horses. *Int J Parasitol* **45**, 237–42 (2015).
679 12. Scheuerle, M. C., Stear, M. J., Honeder, A., Becher, A. M. & Pfister, K. Repeatability of
680 strongyle egg counts in naturally infected horses. *Vet Parasitol* **228**, 103–107 (2016).
681 13. Gold, S. *et al.* Quantitative genetics of gastrointestinal strongyle burden and associated
682 body condition in feral horses. *Int. J. Parasitol. Parasites Wildl.* **9**, 104–111 (2019).
683 14. Sallé, G. *et al.* A genome scan for QTL affecting resistance to Haemonchus contortus in
684 sheep. *J Anim Sci* **90**, 4690–705 (2012).
685 15. Kemper, K. E. *et al.* The distribution of SNP marker effects for faecal worm egg count in
686 sheep, and the feasibility of using these markers to predict genetic merit for resistance
687 to worm infections. *Genet Res Camb* **93**, 203–19 (2011).
688 16. McRae, K. M., McEwan, J. C., Dodds, K. G. & Gemmell, N. J. Signatures of selection in
689 sheep bred for resistance or susceptibility to gastrointestinal nematodes. *BMC*
690 *Genomics* **15**, 637 (2014).
691 17. Sallé, G. *et al.* Functional investigation of a QTL affecting resistance to Haemonchus
692 contortus in sheep. *Vet Res* **45**, 68 (2014).
693 18. Terefe, G. *et al.* Immune response to Haemonchus contortus infection in susceptible

694 (INRA 401) and resistant (Barbados Black Belly) breeds of lambs. *Parasite Immunol.* **29**,
695 415–424 (2007).
696 19. Slusarewicz, P. *et al.* Automated parasite faecal egg counting using fluorescence
697 labelling, smartphone image capture and computational image analysis. *Int J Parasitol*
698 **46**, 485–93 (2016).
699 20. Relf, V. E., Morgan, E. R., Hodgkinson, J. E. & Matthews, J. B. A questionnaire study on
700 parasite control practices on UK breeding Thoroughbred studs. *Equine Vet J* **44**, 466–71
701 (2012).
702 21. Lester, H. E. *et al.* A cost comparison of faecal egg count-directed anthelmintic delivery
703 versus interval programme treatments in horses. *Vet Rec* **173**, 371 (2013).
704 22. Sallé, G., Cortet, J., Koch, C., Reigner, F. & Cabaret, J. Economic assessment of FEC-
705 based targeted selective drenching in horses. *Vet Parasitol* **214**, 159–66 (2015).
706 23. Murphy, D. & Love, S. The pathogenic effects of experimental cyathostome infections in
707 ponies. *Vet Parasitol* **70**, 99–110 (1997).
708 24. Andersen, U. V. *et al.* Physiologic and systemic acute phase inflammatory responses in
709 young horses repeatedly infected with cyathostomins and Strongylus vulgaris. *Vet*
710 *Parasitol* **201**, 67–74 (2014).
711 25. Clark, A. *et al.* Strongyle Infection and Gut Microbiota: Profiling of Resistant and
712 Susceptible Horses Over a Grazing Season. *Front. Physiol.* **9**, (2018).
713 26. Peachey, L. E. *et al.* Dysbiosis associated with acute helminth infections in herbivorous
714 youngstock – observations and implications. *Sci. Rep.* **9**, (2019).
715 27. Walshe, N. *et al.* Removal of adult cyathostomins alters faecal microbiota and promotes
716 an inflammatory phenotype in horses. *Int. J. Parasitol.* **49**, 489–500 (2019).
717 28. Daniels, S. P., Leng, J., Swann, J. R. & Proudman, C. J. Bugs and drugs: a systems
718 biology approach to characterising the effect of moxidectin on the horse's faecal
719 microbiome. *Anim. Microbiome* **2**, 38 (2020).

720 29. Wang, Y. *et al.* Systems metabolic effects of a necator americanus infection in Syrian
721 hamster. *J. Proteome Res.* **8**, 5442–5450 (2009).
722 30. Wu, J.-F. *et al.* Metabolic alterations in the hamster co-infected with Schistosoma
723 japonicum and Necator americanus. *Int. J. Parasitol.* **40**, 695–703 (2010).
724 31. Globisch, D. *et al. Onchocerca volvulus* -neurotransmitter tyramine is a biomarker for
725 river blindness. *Proc. Natl. Acad. Sci.* **110**, 4218–4223 (2013).
726 32. Lagatie, O. *et al.* Evaluation of the diagnostic potential of urinary N-Acetyltyramine-O,β-
727 glucuronide (NATOG) as diagnostic biomarker for Onchocerca volvulus infection.
728 *Parasit. Vectors* **9**, 302 (2016).
729 33. The EPIC Consortium *et al.* Dynamic molecular changes during the first week of human
730 life follow a robust developmental trajectory. *Nat. Commun.* **10**, (2019).
731 34. Wannemacher, R. W. Key role of various individual amino acids in host response to
732 infection. *Am. J. Clin. Nutr.* **30**, 1269–1280 (1977).
733 35. Peters, A. *et al.* Metabolites of lactic acid bacteria present in fermented foods are highly
734 potent agonists of human hydroxycarboxylic acid receptor 3. *PLOS Genet.* **15**,
735 e1008145 (2019).
736 36. Husted, A. S., Trauelsen, M., Rudenko, O., Hjorth, S. A. & Schwartz, T. W. GPCR-
737 Mediated Signaling of Metabolites. *Cell Metab.* **25**, 777–796 (2017).
738 37. Iljazovic, A. *et al.* Perturbation of the gut microbiome by Prevotella spp. enhances host
739 susceptibility to mucosal inflammation. *Mucosal Immunol.* **14**, 113–124 (2021).
740 38. Villarino, N. F. *et al.* Composition of the gut microbiota modulates the severity of
741 malaria. *Proc. Natl. Acad. Sci.* **113**, 2235–2240 (2016).
742 39. Ajibola, O. *et al.* Urogenital schistosomiasis is associated with signatures of microbiome
743 dysbiosis in Nigerian adolescents. *Sci. Rep.* **9**, 829 (2019).
744 40. Stolzenbach, S. *et al.* Dietary Inulin and Trichuris suis Infection Promote Beneficial
745 Bacteria Throughout the Porcine Gut. *Front. Microbiol.* **11**, 312 (2020).

746 41. Helmby, H., Takeda, K., Akira, S. & Grencis, R. K. Interleukin (IL)-18 promotes the
747 development of chronic gastrointestinal helminth infection by downregulating IL-13. *J.*
748 *Exp. Med.* **194**, 355–364 (2001).
749 42. Reynolds, L. A. *et al.* MyD88 signaling inhibits protective immunity to the gastrointestinal
750 helminth parasite Heligmosomoides polygyrus. *J Immunol* **193**, 2984–93 (2014).
751 43. Kelly, B. & Pearce, E. L. Amino Assets: How Amino Acids Support Immunity. *Cell Metab.*
752 **32**, 154–175 (2020).
753 44. Wellendorph, P. *et al.* Deorphanization of GPRC6A: A Promiscuous l-α-Amino Acid
754 Receptor with Preference for Basic Amino Acids. *Mol. Pharmacol.* **67**, 589–597 (2005).
755 45. Quandt, D., Rothe, K., Baerwald, C. & Rossol, M. GPRC6A mediates Alum-induced
756 Nlrp3 inflammasome activation but limits Th2 type antibody responses. *Sci. Rep.* **5**,
757 16719 (2015).
758 46. Youm, Y.-H. *et al.* The ketone metabolite β-hydroxybutyrate blocks NLRP3
759 inflammasome-mediated inflammatory disease. *Nat. Med.* **21**, 263–269 (2015).
760 47. Goldberg, E. L. *et al.* β-Hydroxybutyrate Deactivates Neutrophil NLRP3 Inflammasome
761 to Relieve Gout Flares. *Cell Rep.* **18**, 2077–2087 (2017).
762 48. Sina, C. *et al.* G Protein-Coupled Receptor 43 Is Essential for Neutrophil Recruitment
763 during Intestinal Inflammation. *J. Immunol.* **183**, 7514–7522 (2009).
764 49. Wu, S. *et al.* Worm burden-dependent disruption of the porcine colon microbiota by
765 Trichuris suis infection. *PLoS One* **7**, e35470 (2012).
766 50. Jiao, J. *et al.* Shifts in Host Mucosal Innate Immune Function Are Associated with
767 Ruminal Microbial Succession in Supplemental Feeding and Grazing Goats at Different
768 Ages. *Front. Microbiol.* **8**, 1655 (2017).
769 51. Heeb, L. E. M., Egholm, C., Impellizzieri, D., Ridder, F. & Boyman, O. Regulation of
770 neutrophils in type 2 immune responses. *Curr. Opin. Immunol.* **54**, 115–122 (2018).
771 52. Allen, J. E., Sutherland, T. E. & Rückerl, D. IL-17 and neutrophils: unexpected players in

772 the type 2 immune response. *Curr. Opin. Immunol.* **34**, 99–106 (2015).
773 53. Sorobetea, D., Svensson-Frej, M. & Grencis, R. Immunity to gastrointestinal nematode
774 infections. *Mucosal Immunol.* **11**, 304–315 (2018).
775 54. Michels, C. E. *et al.* Neither interleukin-4 receptor α expression on CD4 $^{+}$ T cells, or
776 macrophages and neutrophils is required for protective immunity to *Trichinella spiralis*.
777 *Immunology* **128**, e385–e394 (2009).
778 55. Al-Qaoud, K. M. *et al.* A new mechanism for IL-5-dependent helminth control: neutrophil
779 accumulation and neutrophil-mediated worm encapsulation in murine filariasis are
780 abolished in the absence of IL-5. *Int. Immunol.* **12**, 899–908 (2000).
781 56. Bonne-Année, S. *et al.* Human and Mouse Macrophages Collaborate with Neutrophils
782 To Kill Larval Strongyloides stercoralis. *Infect. Immun.* **81**, 3346–3355 (2013).
783 57. Anthony, R. M. *et al.* Memory TH2 cells induce alternatively activated macrophages to
784 mediate protection against nematode parasites. *Nat. Med.* **12**, 955–960 (2006).
785 58. Lavoie-Lamoureux, A. *et al.* IL-4 activates equine neutrophils and induces a mixed
786 inflammatory cytokine expression profile with enhanced neutrophil chemotactic
787 mediator release ex vivo. *Am. J. Physiol.-Lung Cell. Mol. Physiol.* **299**, L472–L482
788 (2010).
789 59. Patel, R. S., Tomlinson, J. E., Divers, T. J., Van de Walle, G. R. & Rosenberg, B. R.
790 Single-cell resolution landscape of equine peripheral blood mononuclear cells reveals
791 diverse cell types including T-bet+ B cells. *BMC Biol.* **19**, 13 (2021).
792 60. Raynaud, J. P. [Study of the efficiency of a quantitative coproscopic technic for the
793 routine diagnosis and control of parasitic infestations of cattle, sheep, horses and
794 swine]. *Ann Parasitol Hum Comp* **45**, 321–42 (1970).
795 61. Bolyen, E. *et al.* Reproducible, interactive, scalable and extensible microbiome data
796 science using QIIME 2. *Nat. Biotechnol.* **37**, 852–857 (2019).
797 62. Martin, M. Cutadapt removes adapter sequences from high-throughput sequencing

798 reads. *EMBnet.journal* **17**, 10 (2011).
799 63. Callahan, B. J. *et al.* DADA2: High-resolution sample inference from Illumina amplicon
800 data. *Nat. Methods* **13**, 581–583 (2016).
801 64. Callahan, B. J., McMurdie, P. J. & Holmes, S. P. Exact sequence variants should replace
802 operational taxonomic units in marker-gene data analysis. *ISME J.* **11**, 2639–2643
803 (2017).
804 65. Jansen, J. J., Hoefsloot, H. C. J., van der Greef, J., Timmerman, M. E. & Smilde, A. K.
805 Multilevel component analysis of time-resolved metabolic fingerprinting data. *Anal.*
806 *Chim. Acta* **530**, 173–183 (2005).
807 66. Smilde, A. K. *et al.* ANOVA-simultaneous component analysis (ASCA): a new tool for
808 analyzing designed metabolomics data. *Bioinforma. Oxf. Engl.* **21**, 3043–3048 (2005).
809 67. Chong, J. *et al.* MetaboAnalyst 4.0: towards more transparent and integrative
810 metabolomics analysis. *Nucleic Acids Res.* **46**, W486–W494 (2018).
811 68. Harrell, F. E. & Dupont, C. *Hmisc: Harrell Miscellaneous*. (2017).
812 69. Rohart, F., Gautier, B., Singh, A. & Lê Cao, K.-A. mixOmics: An R package for 'omics
813 feature selection and multiple data integration. *PLoS Comput. Biol.* **13**, e1005752
814 (2017).
815 70. Singh, A. *et al.* DIABLO: an integrative approach for identifying key molecular drivers
816 from multi-omics assays. *Bioinforma. Oxf. Engl.* **35**, 3055–3062 (2019).

817

818 Acknowledgements

819 This work was funded by an Institut Français du Cheval et de l'Équitation grant. We would
820 like to acknowledge Drs. Sonia Lamandé and Lucie Pellissier for critical comments and
821 discussion on a previous version of the manuscript.

Author contributions

GS: analyzed the data, drafted the manuscript. CC: ^{1}H-NMR data acquisition and annotation. JC, CK, JM: sampling and parasitological data acquisition. FR: pony management and sampling. MR, NP: haematological and biochemistry data acquisition. AB: raised funding, project management. NM: analyzed the data, drafted the manuscript.

Competing interest

The author(s) declare no competing interests.

Figure captions

Figure 1. FEC-informed pony potential prediction is robust through time

The distribution of observed Faecal Egg Counts before the experiment (2010-2015), during the experiment (2015) and after the experiment (2015-2020) in the predicted susceptible (8 individuals, 271 records; green) and resistant (9 individuals, 223 records; purple) ponies and their herd unselected counterparts (127 individuals, 1,436 measures; grey) is represented. Dots stand for individual measures and boxplots represent the data distribution (mean materialized by a vertical bar within the box that stands for the 25% to 75% interquartile range).

Figure 2. Representative ^{1}H-NMR spectra measured in resistant and susceptible ponies

Group average ^{1}H-NMR signal intensities are plotted against the considered chemical shifts ranging from 0.995 to 8.995 ppm and overlaid for resistant (TR; purple) and susceptible (TS; green) pony groups at day 0 (strongyle-free; panel a) or day 132 (strongyle infected; panel b). Differential intensity between groups is drawn in red. Associated metabolites are annotated by numbers.

Figure 3. Differential metabolites between infected resistant and susceptible ponies (day 132)

Panel a shows metabolite signal intensity distribution in each pony susceptibility group (purple: resistant, TR; green: susceptible, TS) at day 132. Panel b shows the relationship between these metabolite signal intensities (X-axis) at day 0, and matching log-transformed Faecal Egg Count (Y-axis) at day 132. Panel c describes observed phenylalanine levels in the faecal matter of an independent cohort of British horses with low or high FEC.

Figure 4. Circos plot showing features best discriminating between infected resistant and susceptible ponies (day 132)

For each of the three input data types (clinical data in yellow, bacterial genera in purple and metabolite signals in orange), the features best discriminating between resistant and susceptible ponies are listed. A link is materialized between two features if their shared correlation is above 0.45 (chocolate if positive, grey otherwise). External green and purple lines represent the relative feature level in each pony susceptibility group (resistant, TR: purple; susceptible, TS: green). MGV: Mean Globular Volume; TP: Total Protein; ALP: Alkaline Phosphatase; U14, U25: Unknown metabolites 14 and 25.

Figure 5. Validation of the most discriminant features between resistant and susceptible ponies under strongylid infection

Each row presents the feature level in resistant and susceptible ponies (left panels) and the association with Faecal Egg Count recorded in an independent set of ponies or horses (for the *Prevotella* genus). CLR: Centered Log-Transformed. The figure highlights the significant positive relationship between circulating monocyte count and faecal abundance of the *Prevotella* genus in independent individuals.

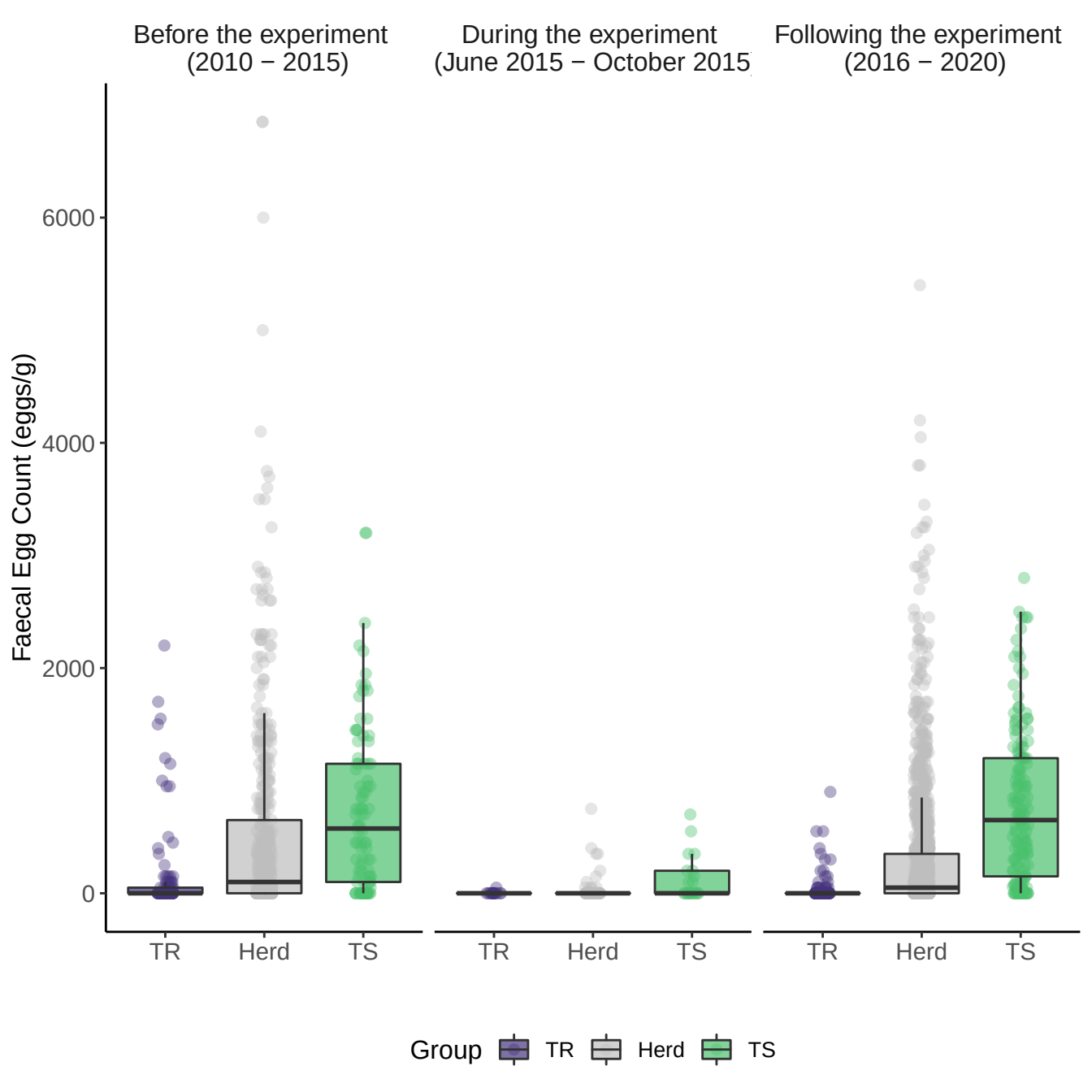
Before the experiment
(2010 − 2015)
During the experiment
(June 2015 − October 2015)
Following the experiment
(2016 − 2020)
Faecal Egg Count (eggs/g)
6000
4000
2000
0
TR
Herd
TS
Group
TR
Herd
TS

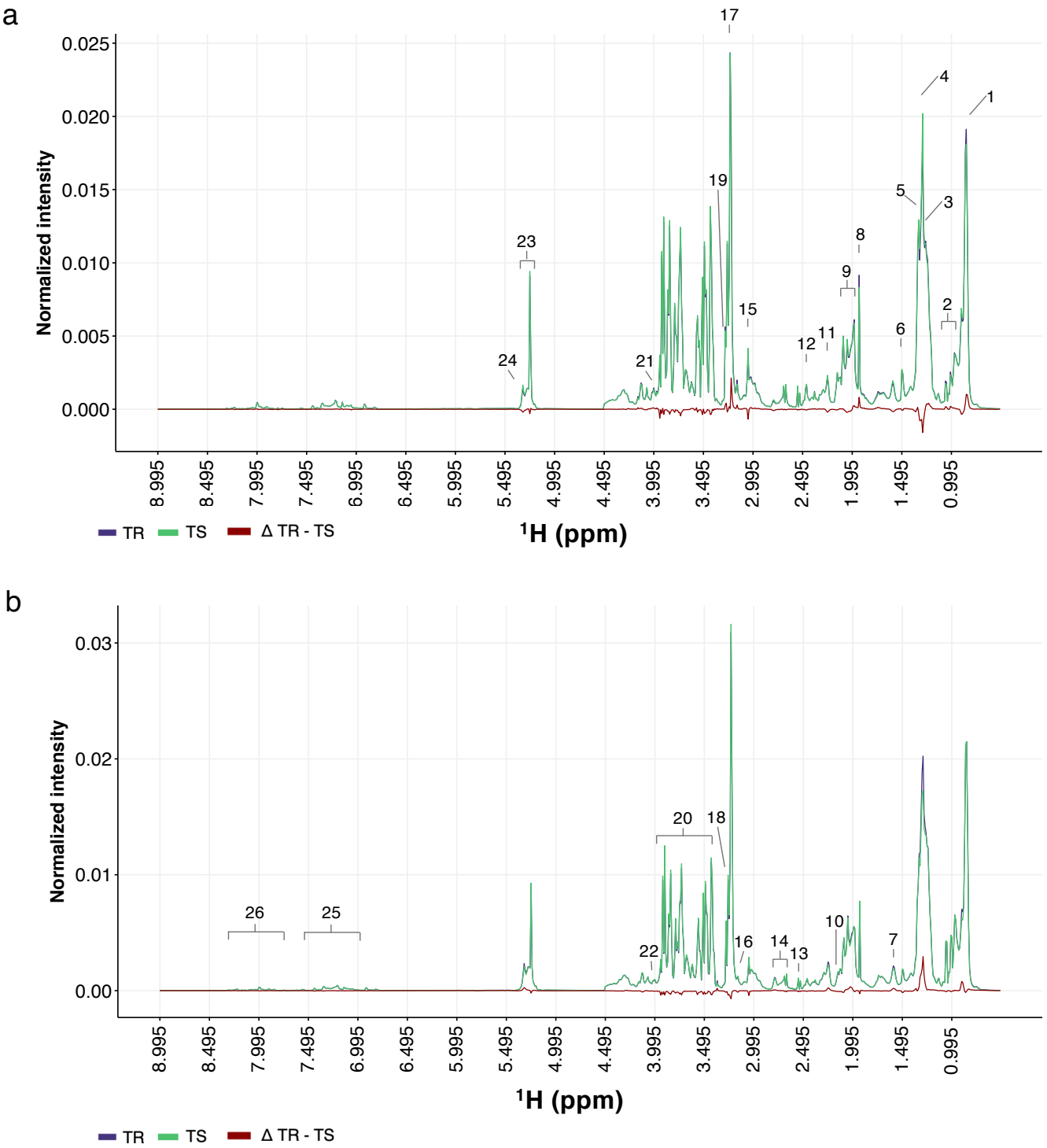

1: Methyl moieties from FA
2: BCAAs (valine, leucine, *iso*-leucine)
3: 3-OH-butyrate
4: Methylene moieties from FA
5: Lactate
6: Alanine
7: Unknown lipid
8: Acetate
9: Acetaminde
10: Glutamine
11: Acetone
12: Pyruvate
13: Citrate
14: Unknown lipid
15: Creatine
16: Dimethyl sulfone
17: Choline containing compounds
18: TMAO
19: Glucose-Betaine
20: Glucose
21: Serine
22: Choline
23: Glusoe
24: Alkalene moieties from FA
25: Tyrosine and phenylalanine
26: Histidine

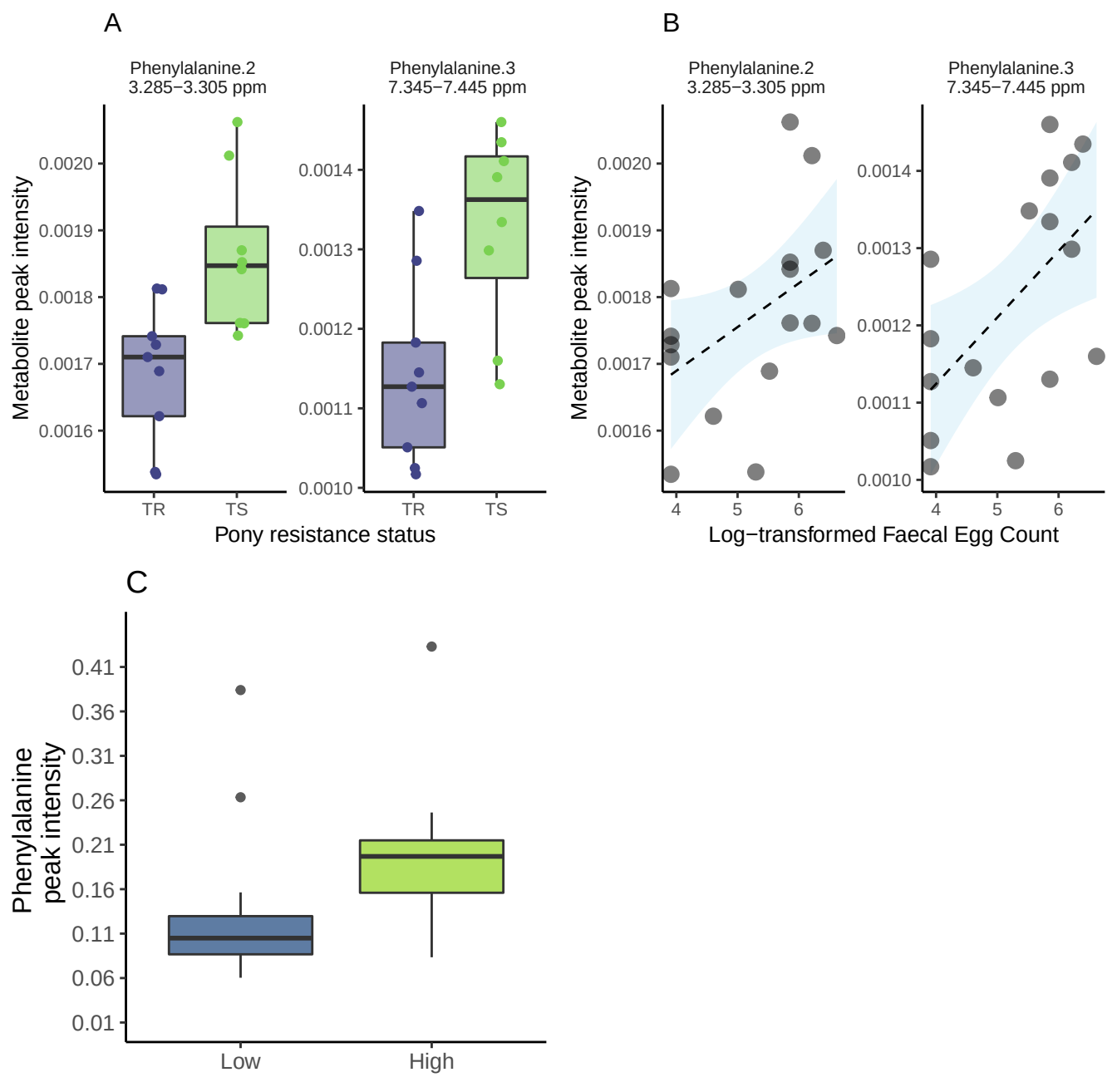
A
Phenylalanine.2
3.285−3.305 ppm
Phenylalanine.3
7.345−7.445 ppm
Metabolite peak intensity
0.0020
0.0019
0.0018
0.0017
0.0016
0.0014
0.0013
0.0012
0.0011
0.0010
TR
TS
Pony resistance status
B
Log−transformed Faecal Egg Count
4
5
6
C
Phenylalanine
peak intensity
0.41
0.36
0.31
0.26
0.21
0.16
0.11
0.06
0.01
Low
High

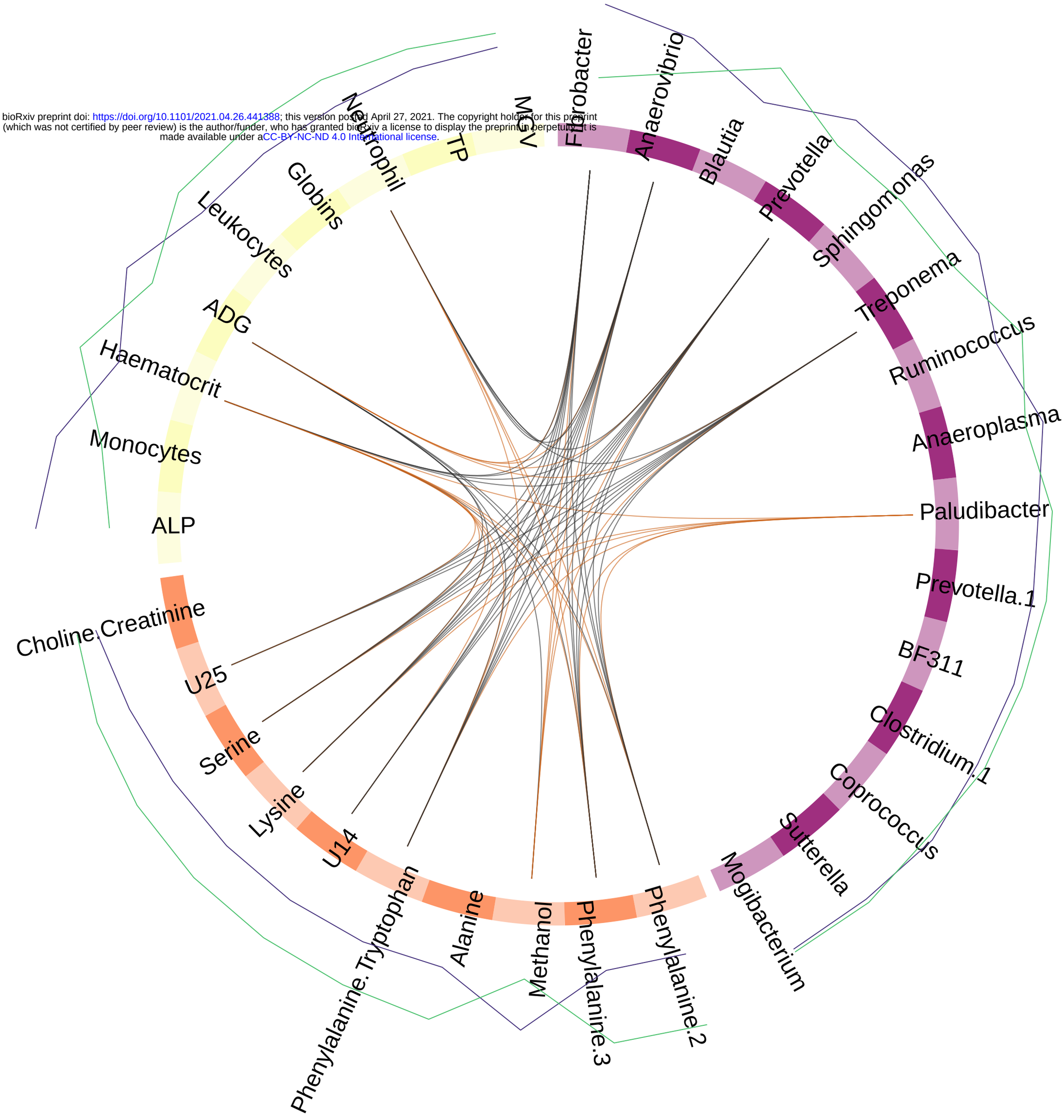

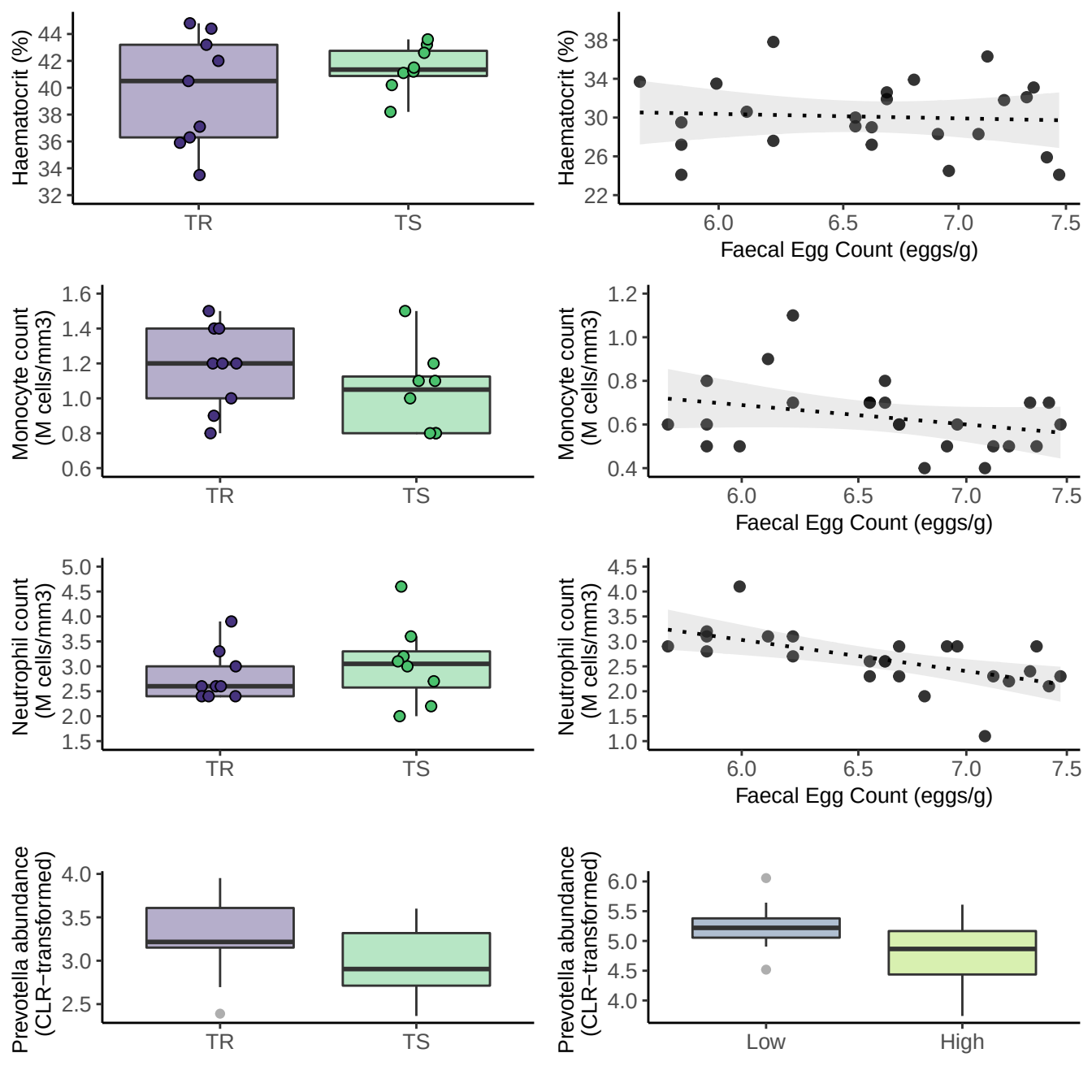
Haematocrit (%)
44
42
40
38
36
34
32
TR
TS
Haematocrit (%)
38
34
30
26
22
6.0
6.5
7.0
7.5
Faecal Egg Count (eggs/g)
Monocyte count (M cells/mm3)
1.6
1.4
1.2
1.0
0.8
0.6
TR
TS
Monocyte count (M cells/mm3)
1.2
1.0
0.8
0.6
0.4
6.0
6.5
7.0
7.5
Faecal Egg Count (eggs/g)
Neutrophil count (M cells/mm3)
5.0
4.5
4.0
3.5
3.0
2.5
2.0
1.5
TR
TS
Neutrophil count (M cells/mm3)
4.5
4.0
3.5
3.0
2.5
2.0
1.5
1.0
6.0
6.5
7.0
7.5
Faecal Egg Count (eggs/g)
Prevotella abundance (CLR−transformed)
4.0
3.5
3.0
2.5
TR
TS
Prevotella abundance (CLR−transformed)
6.0
5.5
5.0
4.5
4.0
Low
High

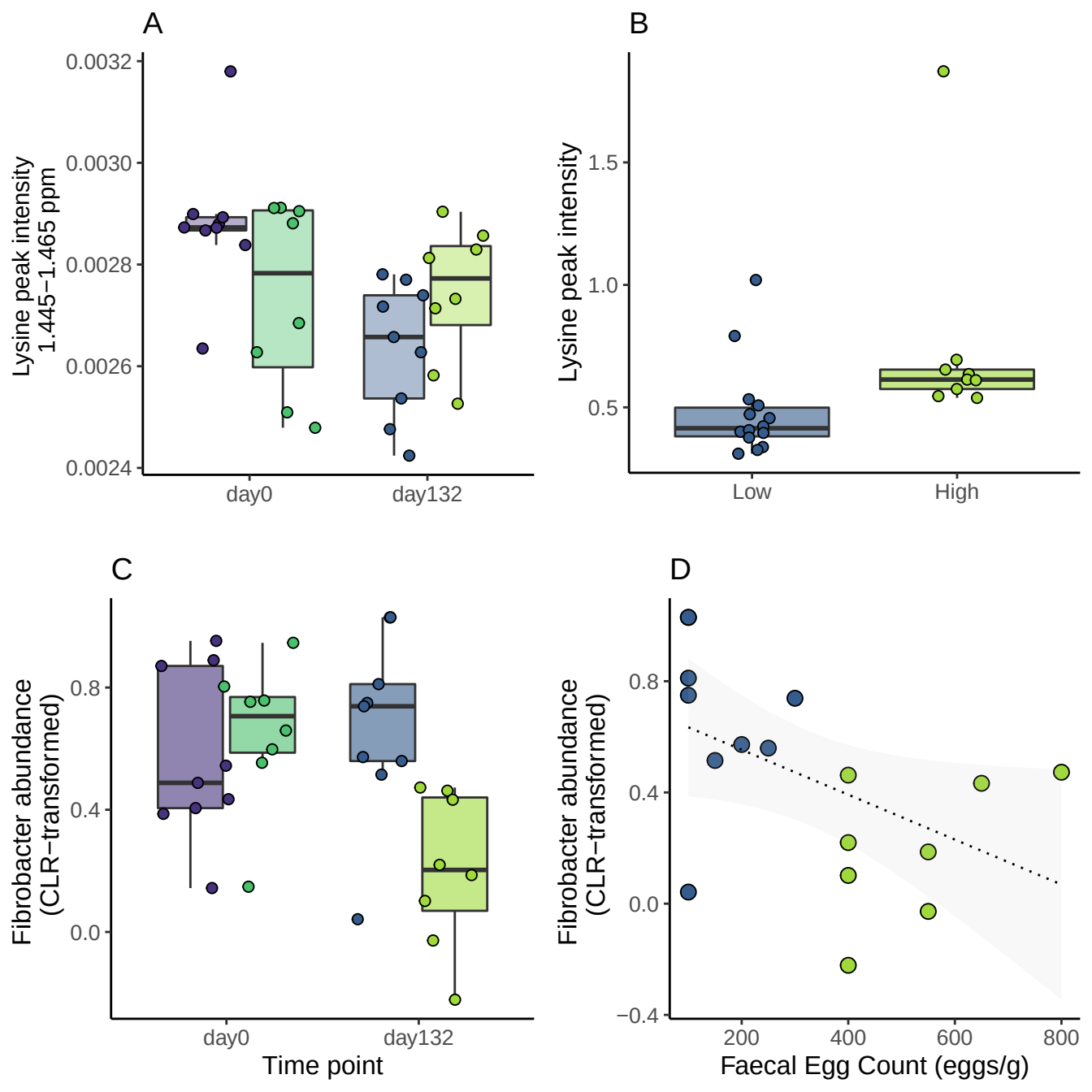
A
Lysine peak intensity
1.445−1.465 ppm
0.0032
0.0030
0.0028
0.0026
0.0024
day0
day132
B
Lysine peak intensity
1.5
1.0
0.5
Low
High
C
Fibrobacter abundance
(CLR−transformed)
0.8
0.4
0.0
day0
day132
Time point
D
Fibrobacter abundance
(CLR−transformed)
0.8
0.4
0.0
−0.4
200
400
600
800
Faecal Egg Count (eggs/g)